RESEARCH ARTICLE

The Arabidopsis receptor kinase STRUBBELIG regulates the response to cellulose deficiency

Ajeet Chaudhary[1], Xia Chen[1], Jin Gao[1], Barbara Leśniewska[1], Richard Hammerl[2], Corinna Dawid[2], Kay Schneitz[1]*

1 Plant Developmental Biology, TUM School of Life Sciences, Technical University of Munich, Freising, Germany, 2 Chair of Food Chemistry and Molecular Sensory Science, TUM School of Life Sciences, Technical University of Munich, Freising, Germany

* kay.schneitz@tum.de

Abstract

Plant cells are encased in a semi-rigid cell wall of complex build. As a consequence, cell wall remodeling is essential for the control of growth and development as well as the regulation of abiotic and biotic stress responses. Plant cells actively sense physico-chemical changes in the cell wall and initiate corresponding cellular responses. However, the underlying cell wall monitoring mechanisms remain poorly understood. In Arabidopsis the atypical receptor kinase STRUBBELIG (SUB) mediates tissue morphogenesis. Here, we show that *SUB*-mediated signal transduction also regulates the cellular response to a reduction in the biosynthesis of cellulose, a central carbohydrate component of the cell wall. *SUB* signaling affects early increase of intracellular reactive oxygen species, stress gene induction as well as ectopic lignin and callose accumulation upon exogenous application of the cellulose biosynthesis inhibitor isoxaben. Moreover, our data reveal that *SUB* signaling is required for maintaining cell size and shape of root epidermal cells and the recovery of root growth after transient exposure to isoxaben. *SUB* is also required for root growth arrest in mutants with defective cellulose biosynthesis. Genetic data further indicate that *SUB* controls the isoxaben-induced cell wall stress response independently from other known receptor kinase genes mediating this response, such as *THESEUS1* or *MIK2*. We propose that *SUB* functions in a least two distinct biological processes: the control of tissue morphogenesis and the response to cell wall damage. Taken together, our results reveal a novel signal transduction pathway that contributes to the molecular framework underlying cell wall integrity signaling.

Author summary

Plant cells are encapsulated by a semi-rigid and biochemically complex cell wall. This particular feature has consequences for multiple biologically important processes, such as cell and organ growth or various stress responses. For a plant cell to grow the cell wall has to be modified to allow cell expansion, which is driven by outward-directed turgor pressure generated inside the cell. In return, changes in cell wall architecture need to be monitored by individual cells, and to be coordinated across cells in a growing tissue, for

an organ to attain its regular size and shape. Cell wall surveillance also comes into play in the reaction against certain stresses, including for example infection by plant pathogens, many of which break through the cell wall during infection, thereby generating wall-derived factors that can induce defense responses. There is only limited knowledge regarding the molecular system that monitors the composition and status of the cell wall. Here we provide further insight into the mechanism. We show that the cell surface receptor STRUBBELIG, previously known to control organ development in Arabidopsis, also promotes the cell's response to reduced amounts of cellulose, a main component of the cell wall.

Introduction

Cell-cell communication is essential to regulate cellular behavior during many processes, including growth, development, and stress responses. In plants, the extra-cellular cell wall constitutes a central element of the underlying molecular mechanisms. It is mainly composed of carbohydrates, such as cellulose, hemicellulose, and pectin, and phenolic compounds, including lignin. Moreover, the cell wall also contains a plethora of different cell-wall-bound proteins [1,2]. It imposes restrictions on cell expansion and the movement of cells and serves as a barrier to pathogen attack. The cell wall counteracts turgor-driven growth and thus cell wall remodeling is required for cell expansion [3]. Cell wall fragments released by pathogen-derived lytic enzymes can act as danger signals and elicit plant immunity responses [4]. These observations imply a necessity for plant cells to monitor cell wall integrity (CWI). Such a mechanism would sense any physico-chemical alterations that occurred in the cell wall and elicit a corresponding compensatory and protective cellular response [5–8].

Little is known about the molecular mechanisms that reside at the nexus of monitoring the cell wall status and the control of development and stress responses. Only a few cell surface signaling factors are presently implicated in monitoring CWI [5,8,9]. For example, a complex between RECEPTOR-LIKE PROTEIN44 (RLP44) and BRASSINOSTEROID INSENSITIVE1 (BRI1), the brassinosteroid receptor, specifically connects BRI1-mediated signaling to the detection of pectin modifications [10,11]. In addition, members of the *Catharanthus roseus* Receptor-like Kinase1-like (CrRLK1L) family of receptor kinases (RKs) are implied in CWI signaling. Recent evidence indicates that a cell wall sensing mechanism depending on a complex between FERONIA (FER) [12] and extracellular leucine-rich repeat extensins (LRXs) negatively regulates vacuole size [13]. Interestingly, the extracellular domain of FER binds pectin in vitro and *FER* is also required to prevent cell bursting upon exposure of root cells to salt [14]. Signaling mediated by ANXUR1 (ANX1) and ANX2 appears to contribute to monitoring cell wall integrity and the prevention of the premature burst of pollen tubes [15–18]. ERULUS (ERU), a CrRLK1L family member with a role in root hair growth regulation [19,20], was shown to be involved in cell wall remodeling during root hair expansion [21].

Plant cells also respond to changes in cellulose levels in the cell wall. Cellulose is present in the form of microfibrils that constitute the main load-bearing elements resisting turgor pressure. The microfibrils are embedded in matrix polysaccharides, mainly various hemicelluloses and pectins [1,2]. Cellulose is synthesized by cellulose synthase (CESA) complexes at the plasma membrane (PM) [22]. The effects of a reduced production of cellulose on plant growth and development can be studied by analyzing mutants with defects in genes encoding CESA subunits involved in primary cell wall biosynthesis [23–27]. Alternatively, pharmacological approaches can be applied. The herbicide isoxaben is a well-characterized inhibitor of cellulose

biosynthesis [28,29]. A number of findings suggest CESAs to be the direct targets of isoxaben. First, several known isoxaben-resistant mutants carry mutations near the carboxyl terminus of certain CESA subunits [30,31]. Second, isoxaben induces a rapid clearing of CESA complexes from the PM [32]. Third, isoxaben uptake or detoxification appears unaffected in resistant plants [33].

The reaction of liquid culture-grown seedlings to isoxaben-induced cellulose biosynthesis inhibition (CBI) represents a thoroughly studied stress response to cell wall damage (CWD) [34–37]. The response is sensitive to osmotic support and eventually includes the upregulation of stress response genes, the production of reactive oxygen species (ROS), an accumulation of phytohormones, such as jasmonic acid (JA), changes in cell wall composition, including the production of ectopic lignin and callose, and finally growth arrest. Similar effects were also observed when studying the phenotypes of different *cesA* mutants [23–27].

The mechanism controlling the CWD response to CBI is known to involve three RKs [34]. THESEUS1 (THE1), another member of the CrRLK1L family, was first implicated in this process [38]. *THE1* was identified based on its genetic interaction with *PROCUSTE1* (*PRC1*), a gene encoding a CESA6 subunit [27]. Amongst others, cellulose-deficient *prc1* single mutants exhibit reduced hypocotyl length and ectopic lignin accumulation. In *the1 prc1* double mutants these effects are ameliorated although cellulose levels remain reduced [38]. Moreover, *THE1* is required for the altered expression levels of several stress-response genes upon exposing liquid-grown seedlings to isoxaben [39]. Recently, the leucine-rich repeat (LRR)-XIIb family RK MALE DISCOVERER1-INTERACTING RECEPTOR LIKE KINASE 2/LEUCINE-RICH REPEAT KINASE FAMILY PROTEIN INDUCED BY SALT STRESS (MIK2/LRR-KISS) [40,41] and the LRR-XIII family member FEI2 [42] have also been shown to participate in the isoxaben-induced cell wall stress response [34,39,43]. Genetic analysis revealed that *THE1* and *MIK2* have overlapping but also distinct functions, suggesting a complex regulation of the CBI response, with *THE1* and *MIK2* promoting this response via different mechanisms. *FEI2* appears to be part of the *THE1* genetic pathway [34].

Tissue morphogenesis in Arabidopsis requires signaling mediated by the atypical LRR-RK STRUBBELIG (SUB). SUB, also known as SCRAMBLED (SCM), is a member of the LRR-V family of RKs and controls several developmental processes, including floral morphogenesis, integument outgrowth, leaf development and root hair patterning [44–46]. SUB represents an atypical receptor kinase, as its *in vivo* function does not require enzymatic activity of its kinase domain [44,47]. Our previous studies indicate that SUB not only localizes to the PM but is also present at plasmodesmata (PD), channels interconnecting most plant cells [48,49], where it physically interacts with the PD-specific C2 domain protein QUIRKY (QKY) [50].

Current data also associate *SUB* signaling to cell wall biology. For example, whole-genome transcriptomics analysis revealed that many genes responsive to *SUB*-mediated signal transduction relate to cell wall remodeling [51]. Moreover, Fourier-transform infrared spectroscopy (FTIR)-analysis indicated that flowers of *sub* and *qky* mutants share overlapping defects in cell wall biochemistry [52]. Thus, apart from functionally connecting RK-mediated signal transduction and PD-dependent cell-cell communication *SUB* signaling also relates to cell wall biology.

Here, we report on a further exploration of the connection between the cell wall and SUB function. Our data reveal a novel role for *SUB* signaling in the CBI-induced CWD response. We show that *SUB* affects several processes, such as ROS accumulation, stress gene induction as well as ectopic lignin and callose accumulation, that are initiated upon application of exogenous isoxaben. Moreover, *SUB* signaling is necessary for maintaining cell shape and recovery of root growth after transient exposure to isoxaben. Our genetic data further indicate that *SUB*, *THE1*, and *MIK2* act in different pathways and that not all contributions of *SUB* to CBI-induced CWD signaling require *QKY* function.

Results

In light of the connection between SUB signaling and cell wall biology, we set out to address if *SUB* plays a role in the seedling responses to cell wall stress. In particular, we focused on the possible role of *SUB* in the isoxaben-induced CWD response.

SUB does not affect cellulose production

We first investigated if *SUB* influences cellulose biosynthesis in seven days-old seedlings. *CESA1*, *CESA3* and *CESA6* genes encode the CESA isoforms present in CSCs of the primary cell wall [53,54]. We first analyzed transcript levels of *CESA1*, *CESA3*, and *CESA6* in wild-type and different *sub* mutants. We could not detect differences in transcript levels of *CESA1*, *CESA3*, and *CESA6* between *sub* and wild type in quantitative real-time polymerase chain reaction (qPCR) experiments (Fig 1A). Moreover, we assessed the levels of cellulose. To this end we generated a predicted null allele of *SUB*, *sub-21*, by a CRISPR-based approach to have available two independent strong *sub* alleles in the Col-0 background (*sub-21*, *sub-9*; see Materials and methods). We did not detect differences between several *sub* mutants and wild type (Fig 1B). However, we could observe a reduction in cellulose levels in plants with a defect in *CESA6* (*prc1-1*) that was comparable to previous findings [27] (Fig 1B). The results indicate that *SUB* does not play a central role in cellulose biosynthesis in seedlings.

SUB affects the isoxaben-induced CWD response

We then assessed if *SUB* activity is necessary for accumulation of reactive oxygen species (ROS) in response to isoxaben-induced CWD. To this end we exposed seven-day wild-type and *sub-9* seedlings, grown on half-strength Murashige and Skoog (MS) plates containing one percent sucrose, to 600 nM isoxaben in a time-course experiment. Seedlings were monitored for up to 120 minutes, at 30 minutes intervals. Upon treatment we assessed fluorescence intensity of the intracellular ROS probe H_2DCFDA in roots [55,56]. In wild-type Col-0 seedlings treated for 30 minutes with isoxaben, we noticed an increase in H_2DCFDA signal compared with mock-treated seedlings (Fig 2A and 2B). Signal intensity of the probe increased further in seedlings exposed to isoxaben for 60 minutes. This signal intensity remained for up to 120 minutes of continuous exposure to isoxaben. In *sub-9* seedlings we detected a slightly and statistically insignificant increased H_2DCFDA signal after 60 to 90 minutes of exposure to isoxaben (Fig 2A and 2B). However, signal intensity was noticeably reduced in comparison to wild type. In comparison to the mock control, isoxaben-treated *sub-9* seedlings continued to show slightly enhanced signal intensity for up to 120 minutes of exposure, although the relative difference to signal levels of mock-treated seedlings was never as pronounced as in wild type. Thus, in comparison to wild type, *sub-9* mutants showed a delayed onset of H_2CDFDA signal appearance and an overall reduced signal intensity for the time frame analyzed. The results indicate that isoxaben causes the formation of intracellular ROS in roots of treated wild-type seedlings within 30 minutes of application. Moreover, *SUB* affects this ROS response.

Next, we tested if *SUB* activity is required for the transcriptional regulation of several marker genes, known to respond to isoxaben-induced CWD within eight hours [34,37,39]. We performed quantitative real-time polymerase chain reaction (qPCR) experiments using RNA isolated from seven days-old liquid-grown seedlings that had been incubated with 600 nM isoxaben for eight hours (Fig 2C, S1 Fig). We observed that isoxaben-induced upregulation of *CCR1*, *PDF1.2*, and *RBOHD* was attenuated in *sub-21* (Fig 2C) and *sub-9* (S1 Fig) mutants compared to wild type. Moreover, we detected a somewhat enhanced upregulation of *CYP81F2* in isoxaben-treated seedlings in comparison to wild type. We detected a statistically significant alteration in the upregulation of *FRK1* for *sub-21* but not for *sub-9*. We did not
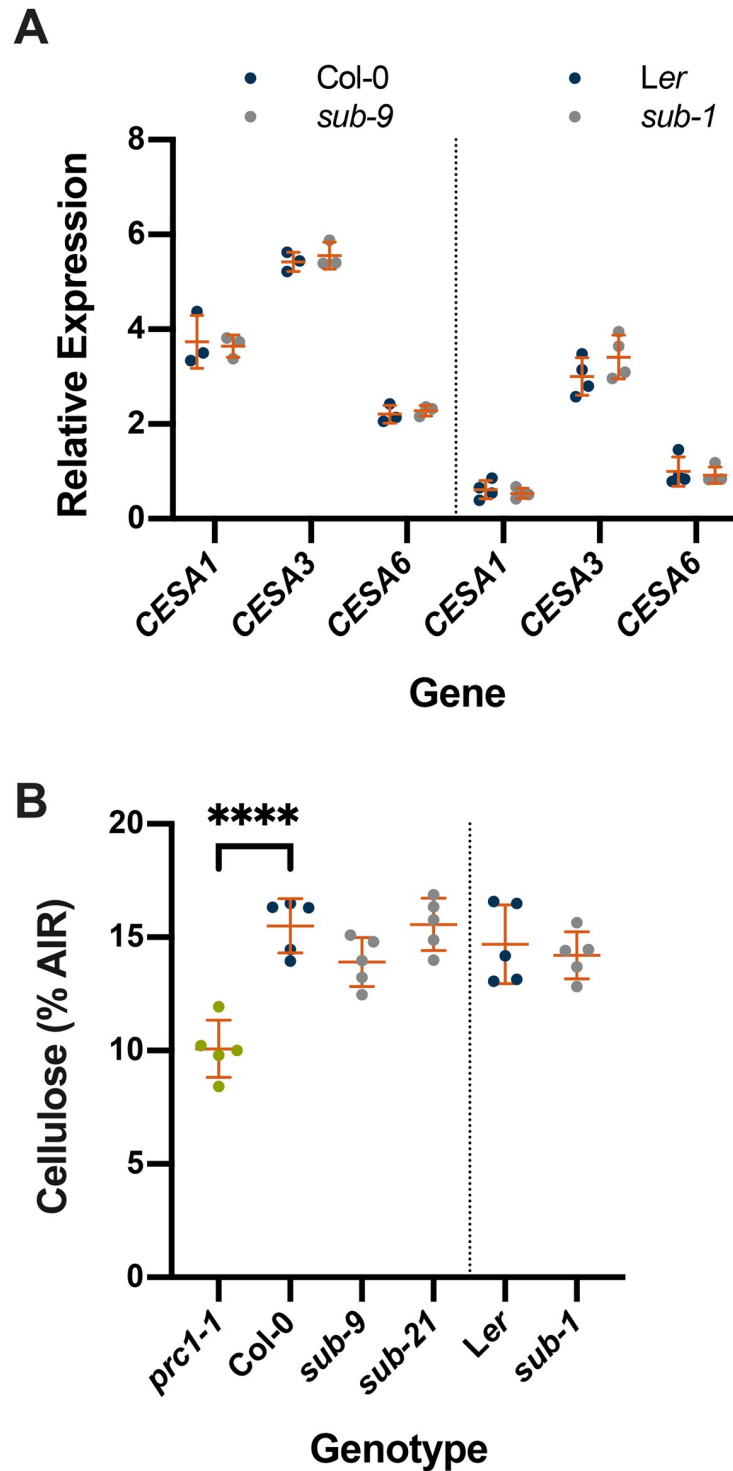
Fig 1. Effects of *SUB* on cellulose content in seven-day-old seedlings. (A) Gene expression levels for primary cell wall *CESA* genes in wild type and *sub* as assessed by qPCR. Individual *CESA* genes and genotypes are indicated. Mean ± SD is shown. Data points designate results of individual biological replicates. For each tested *CESA* gene no statistically significant deviation between wild type and mutant was observed (unpaired t tests, two-tailed P values). The experiment was performed two times with similar results. (B) Estimation of cellulose content. Genotypes are indicated. Data points indicate results of individual biological replicates. Mean ± SD is shown. Col, *sub-9*, *sub-21*, *prc1-1*: asterisks represent adjusted P value (**** P < 0.0001; one-way ANOVA followed by Tukey's multiple comparison tests). L*er*, *sub-1*: no statistically significant difference (unpaired t test, two-tailed P values). Note absence of significant

differences between wild type and different *sub* mutants. The *prc1-1* mutant shows the expected reduction in cellulose content [27]. The experiment was repeated three times with similar results.

observe an effect of *SUB* on *TCH4* induction by isoxaben (Fig 2C, S1 Fig). These results indicate that *SUB* affects the isoxaben-induced upregulation of expression of several marker genes.

The seedlings' response to isoxaben also includes the accumulation of the phytohormone JA [37]. We thus tested if *SUB* affects the isoxaben-induced production of JA in seven days-old liquid-grown seedlings that had been incubated in 600 nM isoxaben for seven hours. We found that JA accumulation appeared largely unaffected in *sub-9* or *sub-21* mutants while two overexpressing lines (pUBQ::SUB:mCherry, Lines O3 and L1, (S2 Fig)) showed strongly diminished JA levels following isoxaben treatment (Fig 2D). The results indicate that *SUB* is not required for isoxaben-induced JA accumulation. The phenotypes of the loss-of-function and overexpressing mutants are not easy to reconcile with each other rendering an interpretation of the effects on JA accumulation seen in the *SUB* overexpressing lines difficult. Thus, their biological relevance needs to be assessed in further experiments.

Isoxaben-induced CBI eventually results in the alteration of cell wall biochemistry as evidenced by the ectopic accumulation of lignin and callose [37]. To investigate if *SUB* affects lignin biosynthesis, we estimated lignin accumulation in roots using phloroglucinol staining after exposing six-day-old liquid-grown seedlings to 600 nM isoxaben for 12 hours. We observed reduced phloroglucinol staining in the root elongation zone of *sub-1* seedlings in comparison to wild type L*er* indicating less ectopic lignin production (Fig 3A and 3B). We also noticed reduced phloroglucinol signal in *sub-9* seedlings (Col-0 background) although the effect was less prominent. However, in our hands Col-0 wild-type plants exhibited an overall weaker phloroglucinol staining indicating that isoxaben-induced lignin accumulation does not occur to the same level as in L*er* (Fig 3A and 3B). We could detect increased phloroglucinol staining in two *pUBQ::SUB:mCherry* lines (L1, O3) (Fig 3A and 3B).

Isoxaben-treatment for 24 hours results in the formation of callose in cotyledons of wild-type seedlings [37]. Thus, we tested if *SUB* is required for this process as well. To this end we transferred seven days-old plate-grown seedlings to liquid medium without isoxaben for 12 hours. Subsequently, medium was exchanged, and seedlings were kept in 600 nM isoxaben for another 24 hours followed by callose detection using aniline blue staining [57]. As expected, we observed prominent aniline blue staining in cotyledons of L*er* and Col wild-type seedlings upon isoxaben treatment (Fig 3C and 3D). By contrast, we detected strongly reduced aniline blue staining in cotyledons of isoxaben-treated *sub-1* and *sub-4* (both in L*er*) as well as *sub-9* and *sub-21* (both in Col). One of the two *SUB* overexpressors (line L1) showed statistically significant stronger aniline blue staining compared to wild type upon application of isoxaben (Fig 3C and 3D).

Taken together, the results indicate that *SUB* is required for the isoxaben-induced formation of lignin and callose in seedlings.

The *SUB*-mediated CBI response is sensitive to sorbitol

The isoxaben-induced CWD response is sensitive to turgor pressure, as indicated by the suppression of lignin or callose accumulation in the presence of osmotica, such as sorbitol [34,36,37]. To test if *SUB* affects a turgor-sensitive CBI response we compared isoxaben-induced accumulation of lignin and callose in six days-old Col-0, *sub-9*, and *pUBQ::SUB:mCherry* seedlings in co-treatments with 600 nM isoxaben and 300 mM sorbitol (Fig 4A–4C). We observed that simultaneous application of isoxaben and sorbitol resulted in strongly
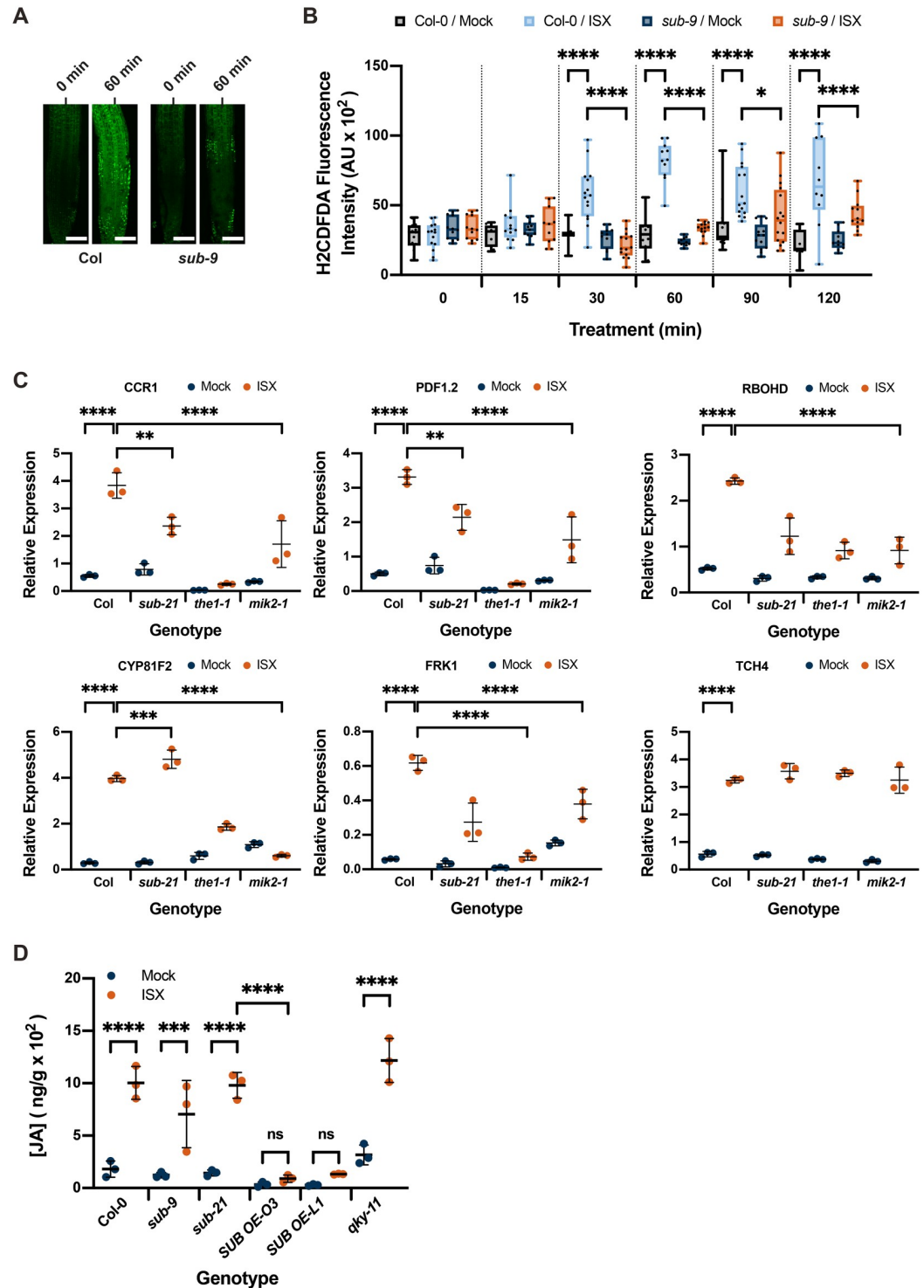
Fig 2. *SUB* effects on isoxaben-induced ROS production, marker gene expression and JA accumulation. (A) Confocal micrographs showing H_2CDFDA signal in root tips of six-day-old seedlings exposed to 600 nM isoxaben for the specified time. Genotypes are indicated. Note reduced signal in *sub-9*. (B) Quantification of results depicted in (A). Genotypes are indicated. Box and whisker plots are shown. Whisker ends mark the minimum and maximum of all the data. $10 \leq n \leq 15$. Asterisks represent adjusted P values (**** $P < 0.0001$; * $P < 0.05$; one-way ANOVA followed by Tukey's multiple comparison tests). No statistically significant differences were measured within or between genotypes during the first 15 minutes of mock or isoxaben treatment or between wild type and *sub-9* mock treatment at any tested time point ($P > 0.9995$; one-way ANOVA followed by Tukey's multiple comparison tests). Experiments were performed three times

with similar results. (C) Gene expression levels of several CBI marker genes by qPCR upon exposure of seven-day-old seedlings to 600 nM isoxaben for eight hours. The results from three biological replicates are shown. Marker genes and genotypes are indicated. Mean ± SD is presented. Asterisks represent adjusted P values (*** $P < 0.0033$, **** $P < 0.0001$, one-way ANOVA followed by Tukey's multiple comparison tests). The experiment was repeated twice with similar results. (D) JA accumulation. Mean ± SD is presented. Genotypes and treatments are indicated. The JA concentration of the isoxaben-treated Col-0, *sub-9*, *sub-21* and *qky-11* mutants did not vary significantly. Asterisks represent adjusted P values (*** $P < 0.001$, **** $P < 0.0001$, ns: not significant; one-way ANOVA followed by Tukey's multiple comparison tests). Experiments were performed three times with similar results. Abbreviation: ISX, isoxaben. Scale bars: (A) 100 μm.

reduced phloroglucinol and aniline blue signal in all tested genotypes, including the SUB: mCherry overexpressing lines, which show hyperaccumulation of lignin or callose if solely isoxaben is applied. Lignin production was undetectable as we could not observe any phloroglucinol staining in main roots of mock/sorbitol or isoxaben/sorbitol-treated seedlings (Fig 4A). Very weak aniline blue signal could be detected in the cotyledons of mock/sorbitol or isoxaben/sorbitol-treated wild-type and mutant seedlings indicating that callose was present at low levels (Fig 4B and 4C). It even appeared that aniline blue-derived signal in the various isoxaben/sorbitol-treated *sub* mutants tended to be even lower when compared to the corresponding mock/sorbitol treatments. The cotyledons of the two mock/sorbitol-treated SUB:mCherry overexpressing lines exhibited low levels of aniline blue staining that that did not change upon exposure to isoxaben/sorbitol. Some of the aniline blue signal differences were statistically significant (for example *sub-9*, adjusted P value < 0.02, and *sub-21*, adjusted P value < 0.0005; one-way ANOVA followed by Tukey's multiple comparison tests). However, given the very low signal levels it is probably unlikely that the differences reflect biological significance.

SUB attenuates isoxaben-induced cell swelling and facilitates root growth recovery

Next, we assessed the biological relevance of *SUB* in the isoxaben-induced CWD response. Exposure of seedlings to isoxaben eventually results in the shortening and swelling of cells of the root epidermis, possibly a result of reduced microfibril formation in the cell wall [34].We transferred six days-old plate-grown seedlings into a mock solution or a solution containing 600 nM isoxaben for up to seven hours. We then assessed the timing of the initial appearance of altered cellular morphology of root epidermal cells. In addition, we monitored the severity of the phenotype. We focused on cells of the elongation zone that bordered the root meristem. Notably, we did not observe any obvious morphological alterations in mock-treated wild-type or mutant seedlings (Fig 5). In Col-0 wild-type seedlings cell shortening and swelling first became noticeable during the five to six-hour interval proceeding treatment (Fig 5) (44/96 seedlings total, n = 4), as reported previously [34]. Upon isoxaben application to *sub-9* or *sub-21* seedlings, however, similar cellular alterations were already detected at the three to four-hour interval post treatment initiation (*sub-9*: 23/57, n = 2; *sub-21*: 20/46, n = 2). In addition, *sub* mutants exhibited more pronounced cellular alterations after seven hours of isoxaben treatment in comparison to wild type (Fig 5).

In wild-type seedlings, a transient 24-hour exposure to isoxaben results in a temporary stop of root growth followed by a rapid recovery [34]. We tested the role of *SUB* in root growth recovery upon a 24 hour-treatment with isoxaben. Six-day-old wild-type and mutant seedlings grown on plates were transferred onto media containing 600 nM isoxaben for 24 hours, then moved to fresh plates lacking isoxaben. Seedlings were then monitored for continued root growth at 24-hour intervals, for a total of 72 hours (Table 1). As control, we used the *ixr2-1* mutant, which is resistant to isoxaben due to a mutation in the *CESA6* gene [30,31,58]. We observed that 98 percent of *ixr2-1* seedlings recovered root growth already within 24 hours,
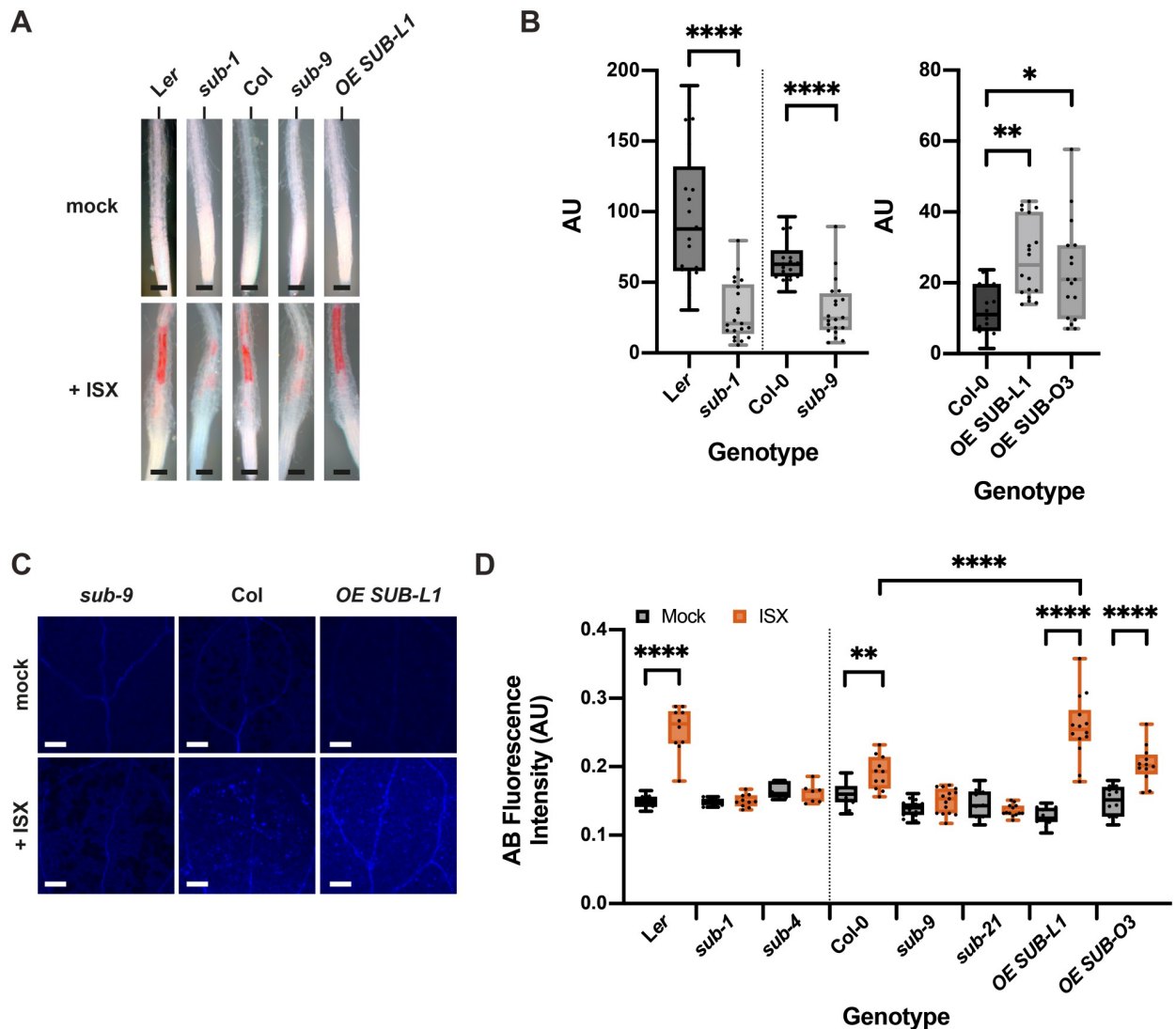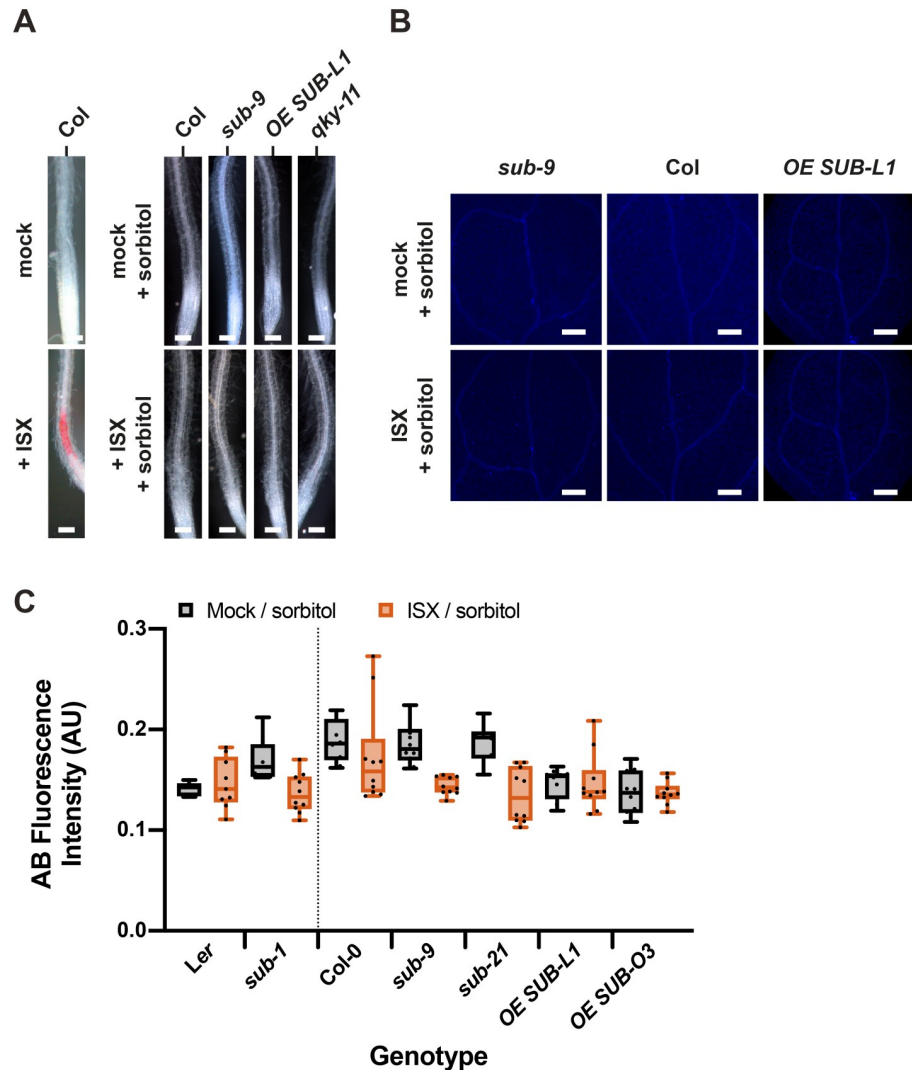
Fig 3. *SUB* affects isoxaben-induced lignin and callose accumulation. (A) Phloroglucinol signal strength indicating lignin accumulation in roots of six-day-old seedlings exposed to 600 nM isoxaben for 12 hours. Genotypes: L*er*, and *sub-1* (L*er*); Col, *sub-9* (Col), *pUBQ::gSUB:mCherry* (line OE SUB L1). (B) Quantification of the results depicted in (A). Left panel shows results obtained from different *sub* mutants in the L*er* or Col background. Right panel depicts results from two independent *pUBQ::gSUB:mCherry* transgenic lines overexpressing *SUB* (Col, lines OE SUB L1, O3). Box and whisker plots are shown. Whisker ends mark the minimum and maximum of all the data. 16 ≤ n ≤ 21. Asterisks represent statistical significance. Left panel: P < 0.0001; unpaired t test, two-tailed P values. Right panel: adjusted P values; * P < 0.03, ** P < 0.002; one-way ANOVA followed by Tukey's multiple comparison tests. The experiment was performed three times with similar results. (C) Confocal micrographs show cotyledons of seven-day-old *sub-9*, Col, and *pUBQ::gSUB:mCherry* (line L1) seedlings treated with mock or 600 nM isoxaben for 24 hours. Aniline blue fluorescence signal strength indicates callose accumulation. (D) Quantification of the results depicted in (C). Left panel shows results obtained from *sub* mutants in L*er* background. Right panel indicates results obtained from *sub* mutants and two independent *pUBQ::gSUB:mCherry* transgenic lines overexpressing *SUB* (lines L1, O3) in Col background. Box and whisker plots are shown. Whisker ends mark the minimum and maximum of all the data. 7 ≤ n ≤ 18. Asterisks represent adjusted P values (** P < 0.002, **** P < 0.0001; one-way ANOVA followed by Tukey's multiple comparison tests). The experiment was performed three times with similar results. Abbreviation: ISX, isoxaben. Scale bars: (A) 0.1 mm; (C) 0.2 mm.

indicating that treatment did not generally impact the seedlings' ability to recover root growth. We then tested wild-type seedlings. We noticed that 46 percent of L*er* and 39 percent of Col seedlings had resumed root growth after 24 hours. By 72 hours, 86 percent of L*er* and 90 percent of Col seedlings had recovered root growth. In contrast, a significantly reduced fraction

Fig 4. The effects of sorbitol on lignin and callose accumulation upon isoxaben exposure. (A) Phloroglucinol signal strength indicating lignin accumulation in roots of six-day-old seedlings exposed to mock/300 mM sorbitol or to 600 nM isoxaben/300 mM sorbitol for 12 hours. Genotypes: Col, *sub-9* (Col), *pUBQ::gSUB:mCherry* (line OE SUB-L1), *qky-11* (Col). Note absence of detectable signal upon simultaneous application of isoxaben and sorbitol. The experiment was performed three times with similar results (n ≥ 10). (B) Confocal micrographs show cotyledons of seven-day-old *sub-9*, Col, and *pUBQ::gSUB:mCherry* (Col, line OE SUB-L1) seedlings treated with mock/300 mM sorbitol or 600 nM isoxaben/300 mM sorbitol for 24 hours. Aniline blue fluorescence signal strength indicates callose accumulation. No increase in signal intensity can be observed in isoxaben-treated seedlings. (C) Quantification of the results depicted in (B). Left panel depicts results obtained from L*er* and *sub-1* (L*er* background). Right panel shows results obtained from Col-0 and *sub* mutants in Col-0 background and also depicts results from two independent *pUBQ::gSUB:mCherry* transgenic lines overexpressing *SUB* (Col, lines SUB OE-L1, SUB OE-O3). Box and whisker plots are shown. Whisker ends mark the minimum and maximum of all the data. 5 ≤ n ≤ 10. The experiment was performed three times with similar results. Abbreviation: ISX, isoxaben. Scale bars: (A) 0.1 mm; (C) 0.2 mm.

of *sub-1* and *sub-4* mutants had resumed root growth when compared to wild-type L*er* (Table 1). The *sub-9* and *sub-21* mutants also showed reduced root growth recovery in comparison to Col although *sub-21* appeared less affected than *sub-9*. Importantly, *ixr2-1 sub-9* mutants behaved identical to *ixr2-1* single mutants at all time points scored. These findings
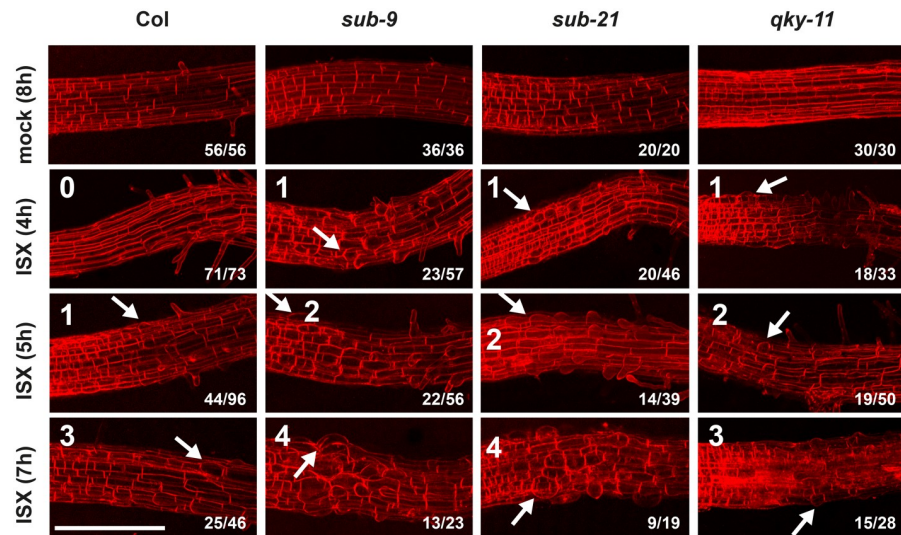
Fig 5. Root epidermal cell shape changes upon isoxaben treatment. Six-day-old seedlings counter-stained with the membrane stain FM4-64 are shown. Confocal micrographs depict the region where the elongation zone flanks the root meristem. Time of exposure in hours to 600 nM isoxaben (ISX) or mock is indicated as are the genotypes. Numbers of roots showing the phenotype are indicated (n/total number of roots scored). Arrows denote aberrant cell shapes. Scale bar: 0.1 mm.

https://doi.org/10.1371/journal.pgen.1008433.g005

indicate that *ixr2-1* is epistatic to *sub-9* and that the observed isoxaben-induced decrease in root growth recovery in *sub-9* mutants relates to the herbicide.

Taken together, the results suggest that *SUB* attenuates cell size and shape changes in root epidermal cells and facilitates root growth recovery during the isoxaben-induced CWD response.

Table 1. Root growth recovery after isoxaben treatment.

Genotype	N total[a]	24 h[b]	48 h[b]	72 h[b]
L*er*	110	45.5	69.1	85.5
sub-1	82	24.4**	50.0*	64.6**
sub-4	76	17.1**	39.5****	52.6****
qky-8	87	37.9ns	64.4ns	88.5ns
Col-0	142	38.7	65.5	90.1
sub-9	88	23.9*	45.5**	70.5**
sub-21	72	26.4ns	51.4ns	68.1**
qky-11	81	37.0ns	64.2ns	92.6ns
ixr2-1	83	97.6****	97.6****	97.6ns
sub-9 ixr2-1	77	100.0****	100.0****	100.0**
the1-1	78	41.0ns	69.2ns	88.5ns

Percentages of root growth recovery of plate-grown, seven-day-old seedlings after transient exposure to 600 nM isoxaben for 24 hours. The top four sample rows list genotypes that are in Ler background. The bottom seven sample rows list genotypes that are in Col background.

[a]Total number of samples. Cases per class and timepoint were pooled from three independent experiments. For each biological replicate $22 \leq n \leq 32$ seedlings were analyzed per genotype and time point.

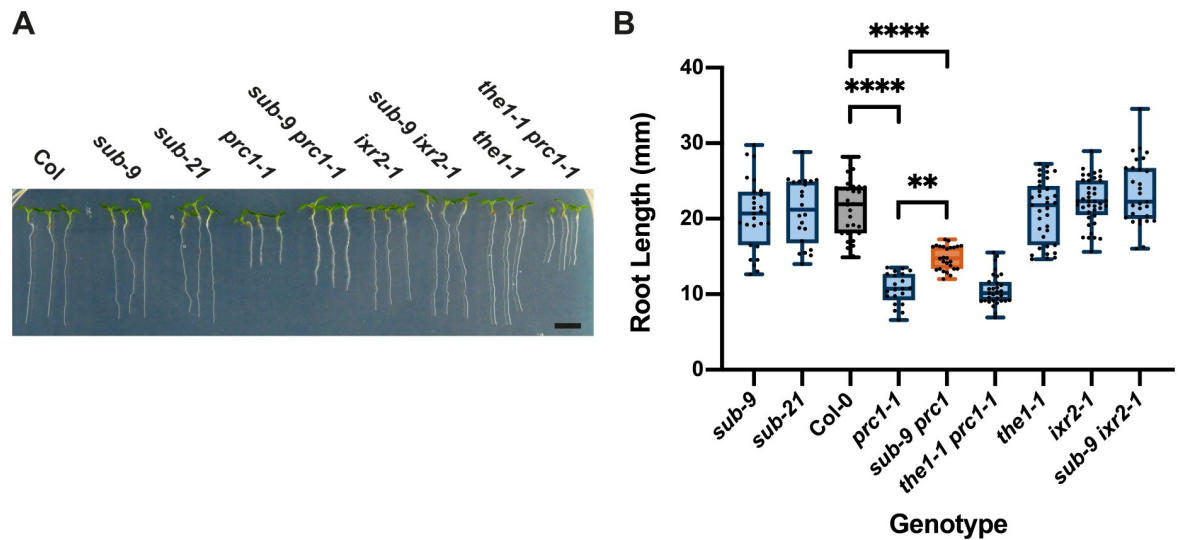[b]Statistical significance (mutant vs respective wild type): na, not applicable;

ns, not significant;

* $P < 0.05$;

** $P < 0.005$;

**** $P < 0.0001$; (Fisher's exact test; two-sided).

https://doi.org/10.1371/journal.pgen.1008433.t001

Fig 6. *SUB* effect on root growth inhibition in *prc1-1*. (A) Root length in seven-day-old seedlings grown on plates under long-day conditions (16 hours light). Genotypes are indicated. Note the partial rescue of root length in *sub-9 prc1-1* but not in *the1-1 prc1-1*. (B) Quantification of the data shown in (A). Box and whisker plots are shown. Whisker ends mark the minimum and maximum of all the data. $21 \leq n \leq 40$. Asterisks represent adjusted P values (** P < 0.004, **** P < 0.0001; one-way ANOVA followed by Tukey's multiple comparison tests). The experiment was performed three times with similar results. Scale bars: 0.5 mm.

https://doi.org/10.1371/journal.pgen.1008433.g006

SUB attenuates root growth in *prc1-1*

PRC1 encodes the CESA6 subunit of cellulose synthase [27] and *prc1* loss-of-function mutants show reduced cellulose levels [27] (Fig 1B). In addition, *prc1-1* mutants are characterized by a reduced elongation of etiolated hypocotyls and roots [27]. To test if *SUB* also affects a biological process in a scenario where cellulose reduction is induced genetically we compared root length in *sub-9*, *sub-21*, and *prc1-1* single and *sub-9 prc1-1* double mutants (Fig 6A and 6B). We found that root length of *sub-9* or *sub-21* did not deviate from wild type while root length of *prc1-1* was markedly smaller in comparison to wild type, confirming previous results [27]. Interestingly, however, we observed that *sub-9 prc1-1* exhibited a significantly longer root than *prc1-1* though *sub-9 prc1-1* roots were still notably smaller than wild type roots. The results indicate that *SUB* contributes to root growth inhibition in *prc1-1*.

SUB and *QKY* contribute differently to the CBI response

Evidence suggests that a protein complex including SUB and QKY is important for SUB-mediated signal transduction regulating tissue morphogenesis [50,59,60]. Thus, we wanted to explore if *QKY* is also required for the isoxaben-induced CWD response in seedlings. We first investigated if *QKY* affects the early isoxaben-induced changes in intracellular ROS levels by assessing H_2CDFDA fluorescence in root tips of *qky-11* seedlings that were treated with 600 nM isoxaben. Similar to wild type we observed an obvious increase in signal intensity between mock and isoxaben-treated *qky-11* (Fig 7A). This indicates that *QKY* does not contribute to altered intracellular ROS levels in root tips of treated seedlings in a noticeable fashion. We then tested if *QKY* promotes isoxaben-induced marker gene expression in liquid-grown seedlings. Using qPCR, we observed that *QKY* did not noticeably affect the expression levels of the tested marker genes (Fig 7B). Next, we assessed isoxaben-induced lignin accumulation in wild-type and *qky* seedlings by phloroglucinol staining. We noticed
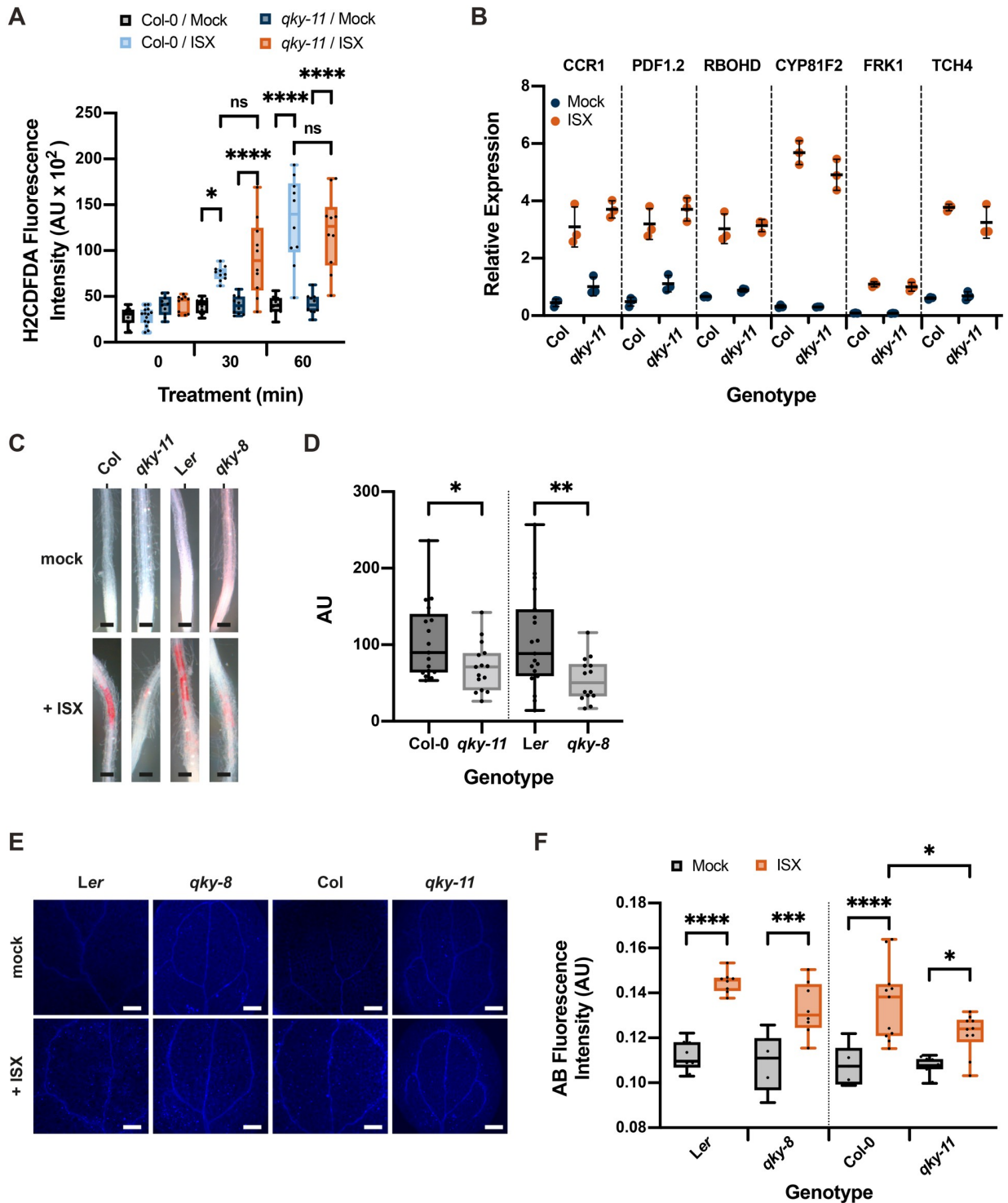
Fig 7. Role of *QKY* in isoxaben-induced CBI responses. (A) Quantification of H₂CDFDA signal indicating ROS accumulation in root tips of six-day-old Col-0 and *qky-11* seedlings exposed to mock or 600 nM isoxaben for the indicated time. Note the high signal in *qky-11* after a 30- or 60-minutes exposure to isoxaben. Box and whisker plots are shown. Whisker ends mark the minimum and maximum of all the data. 10 ≤ n ≤ 14. Asterisks represent adjusted P values (* P < 0.04, **** P < 0.0001; ns: not significant; one-way ANOVA followed by Tukey's multiple comparison tests). No statistically significant differences were measured within or between genotypes at the zero minute time point of mock or isoxaben treatment or between wild-type and *qky-11* mock treatment at the 30 and 60 minutes time points (P > 0.8557; one-way ANOVA followed by Tukey's multiple comparison tests). Experiments were performed three times with similar results. (B) Gene expression levels of several CBI marker genes by qPCR upon exposure of seven-day-old seedlings to 600 nM isoxaben for eight hours. The results from three

biological replicates are shown. Marker genes and genotypes are indicated. Mean ± SD is presented. The experiment was repeated three times with similar results. (C) Phloroglucinol signal strength indicating lignin accumulation in roots of six-day-old seedlings exposed to 600 nM isoxaben for 12 hours. Genotypes: Col, *qky-11* (Col), L*er*, and *sub-1* (L*er*). (D) Quantification of the results depicted in (C). Genotypes are indicated. Box and whisker plots are shown. Whisker ends mark the minimum and maximum of all the data. 15 ≤ n ≤ 19. Asterisks represent statistical significance (∗ P < 0.04, ∗∗ P < 0.01; unpaired t test, two-tailed P values). The experiment was performed three times with similar results. (E) Confocal micrographs show cotyledons of seven-day-old L*er*, *qky-8* (L*er*), Col, and *qky-11* (Col) seedlings treated with mock or 600 nM isoxaben for 24 hours. Aniline blue fluorescence signal strength indicates callose accumulation. (F) Quantification of the results depicted in (E). Left panel shows results obtained from *qky-8* mutants in L*er* background. Right panel indicates results obtained from *qky-11* mutants in Col background. Box and whisker plots are shown. Whisker ends mark the minimum and maximum of all the data. 5 ≤ n ≤ 11. Asterisks represent adjusted P values (∗ P < 0.04, ∗∗∗ P < 0.0005, ∗∗∗∗ P < 0.0001; one-way ANOVA followed by Tukey's multiple comparison tests). The experiment was performed three times with similar results. Abbreviation: ISX, isoxaben. Scale bars: (C) 0.1 mm; (E) 0.2 mm.

https://doi.org/10.1371/journal.pgen.1008433.g007

reduced staining in *qky-8* and *qky-11* mutants compared to wild type (Fig 7C and 7D). Again, the effect was less obvious in Col-0. In addition, we noticed that *qky-11* did not affect the absence of lignin accumulation in seedlings simultaneously treated with isoxaben and sorbitol (Fig 4A). We also investigated the role of *QKY* in isoxaben-induced callose deposition by scoring the aniline blue-derived signal in cotyledons. Similar to wild type we observed a significant difference in signal strength between mock and isoxaben-treated *qky-8* and *qky-11* (Fig 7E and 7F). In addition, we found that *qky-11* seedlings still accumulated increased JA levels upon induction by isoxaben (Fig 2D). The results indicate that *QKY* is required for isoxaben-induced increase in lignin but does not play a role in the accumulation of callose or JA.

Next we analyzed isoxaben-induced shortening and swelling of root epidermal cells in *qky-11* mutants (Fig 4). We noticed the first defects in a three to four-hour interval (18/33, n = 3). Cell swelling after seven hours exposure to isoxaben was prominent in *qky-11* but less severe in comparison to *sub-9* (Fig 4). Finally, we investigated root growth recovery after transient isoxaben application. We observed that *qky-8* and *qky-11* mutants did not significantly deviate from wild type (Table 1).

Taken together, the results indicate that *QKY* and *SUB* contribute to the isoxaben-mediated induction of lignin accumulation. Moreover, *QKY* also plays a role in the suppression of isoxaben-induced alterations in cell morphology in the root epidermis. However, the results also imply that *QKY* is not required for isoxaben-induced early ROS accumulation in root tips, marker gene induction as well as callose accumulation in cotyledons and does not affect root growth recovery after transient exposure to isoxaben.

SUB and *THE1* share partially overlapping functions

THE1 is a central regulator of the isoxaben-induced CBI response [34,39,43]. Our data indicate that *SUB* and *THE1* have overlapping but also distinct functions in this process. For example, *SUB* and *THE1* control isoxaben-induced lignin accumulation in roots (Fig 3) [34,39]. In contrast, we failed to detect an effect of *THE1* on root growth inhibition in *prc1-1*, while *SUB* contributes to this process (Fig 6). In addition, we found that in contrast to *sub* root growth recovery of *the1-1* seedlings upon transient exposure to isoxaben did not deviate from wild type (Table 1).

To explore further the relationship between *THE1* and *SUB* we investigated the requirement of *THE1* for isoxaben-dependent marker gene induction. We observed that like *SUB* *THE1* is required for isoxaben-induced upregulation of *CCR1*, *PDF1.2*, and *RBOHD* although in the case of *CCR1* and *PDF1.2* *the1-1* seedlings show a stronger effect than *sub* mutants (Fig 2C, S1 Fig). Regarding *CYP81F2* we noticed a major difference between *sub* and *the1-1*. While *CYP81F2* appeared slightly higher induced upon exposure to isoxaben in *sub* seedlings (Fig 2C, S1 Fig) we observed strongly reduced *CYP81F2* transcript levels in *the1-1* (Fig 2C). This

observation differs from previous work where *CYP81F2* induction was reported to be unaltered in *the1-1* [39]. We also noticed that *FRK1* induction was strongly reduced in *the1-1* (Fig 2C), confirming previous data [39], while in *sub* seedlings isoxaben-dependent *FRK1* transcript levels were either reduced or unaltered depending on the *sub* allele (Fig 2D, S1 Fig).

Next, we compared the role of *SUB* and *THE1* in etiolated hypocotyl elongation. *THE1* contributes to the reduction of hypocotyl length of cellulose-diminished *prc1-1* seedlings grown in the dark as evidenced by the partial recovery of hypocotyl elongation in *the1 prc1* double mutants [38]. We compared *sub-9 prc1-1* to *the1-1 prc1-1* with respect to hypocotyl elongation in six-day-old etiolated seedlings (Fig 8). We observed strongly reduced hypocotyl elongation in *prc1-1* in comparison to wild type and a significant suppression of this reduction in *the1-1 prc1-1* double mutants (Fig 8A and 8B), as described earlier [38]. In contrast, hypocotyl length in *sub-9* mutants was not decreased, nor was there a partial reversal of reduced hypocotyl
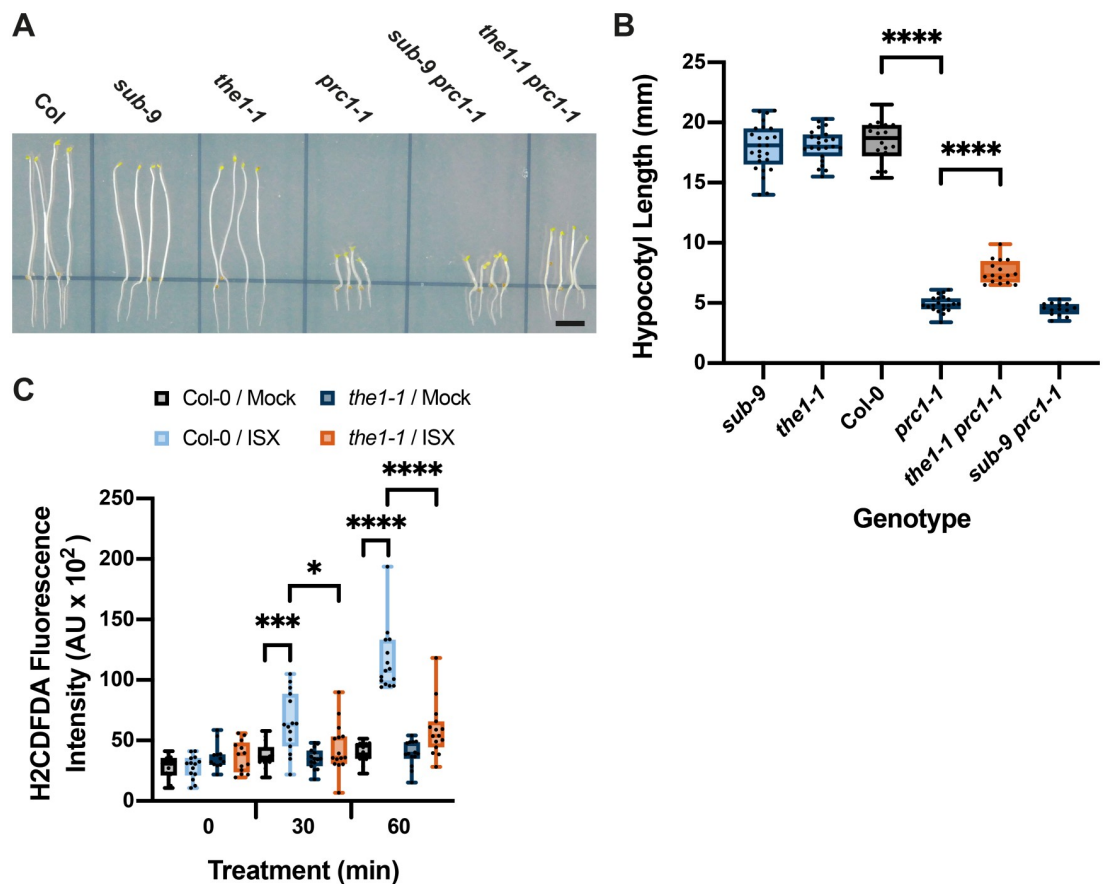
Fig 8. Influence of *THE1* on etiolated hypocotyl length of *prc1-1* and isoxaben-induced ROS accumulation in root tips. (A) Hypocotyl elongation in six-day-old seedlings grown on plates in the dark. Genotypes are indicated. Note the partial rescue of hypocotyl elongation in *the1-1 prc1-1* but not in *sub-9 prc1-1*. (B) Quantification of the data shown in (A). Whisker ends mark the minimum and maximum of all the data. $14 \leq n \leq 25$. Asterisks represent adjusted P values (**** $P < 0.0001$; one-way ANOVA followed by Tukey's multiple comparison tests). The experiment was performed three times with similar results. (C) Quantification of H_2CDFDA signal indicating ROS accumulation in root tips of six-day-old Col-0 and *the1-1* seedlings exposed to mock or 600 nM isoxaben for the indicated time. Note the low signal in *the1-1* after a 30- or 60-minutes exposure to isoxaben. Box and whisker plots are shown. Whisker ends mark the minimum and maximum of all the data. $12 \leq n \leq 15$. Asterisks represent adjusted P values (* $P < 0.05$; *** $P = 0.0005$; **** $P < 0.0001$, one-way ANOVA followed by Tukey's multiple comparison tests). No statistically significant differences were measured within or between genotypes at the zero minute time point of mock or isoxaben treatment or between wild-type and *the1-1* mock treatment at the 30 and 60 minutes time points ($P > 0.7997$; one-way ANOVA followed by Tukey's multiple comparison tests). Experiments were performed three times with similar results. Abbreviation: ISX, isoxaben. Scale bars: 0.5 mm.

https://doi.org/10.1371/journal.pgen.1008433.g008

elongation in *sub-9 prc1-1* double mutants (Fig 8A and 8B). The results indicate that *SUB* does not affect hypocotyl elongation in etiolated wild-type or *prc1-1* seedlings.

Finally, we assessed the role of *THE1* in isoxaben-induced early ROS accumulation in root tips. We noticed no difference in H$_2$CDFDA signal intensity when comparing *the1-1* seedlings that had been treated with either mock or isoxaben for 30 minutes (Fig 8C). By contrast, isoxaben-induced reporter signal in the root tip became slightly stronger than the mock-mediated signal at the 60 minutes time point (Fig 8C). Overall the results resemble the findings obtained with *sub-9* mutants (Fig 2B).

In summary, *SUB* and *THE1* are required for ROS and lignin accumulation in roots. The two genes exhibit partial overlap but also clear distinctions with respect to their role in stress marker gene induction. *SUB* and *THE1* show opposite effects on growth inhibition of roots and hypocotyls in *prc1* mutants and their functions differ with respect to root growth recovery.

Discussion

Cell wall signaling during plant development and stress responses relies on complex and largely unknown signaling circuitry [5,8,9,35,61]. Only a few RKs, including THE1, MIK2, and FEI2, have so far been shown to play a major role in CBI-induced CWD signaling [34,38,39,43]. Our data establish *SUB* signal transduction as a novel component in the molecular framework mediating the CWD response.

To date, published evidence has attributed a developmental role to *SUB*, particularly in the control of tissue morphogenesis and root hair pattern formation [44–46,51,62]. The evidence provided in this work identifies a novel role for *SUB* in CWD signaling. Application of isoxaben results in reduced levels of cellulose [28,29]. Our results indicate that *SUB* affects multiple aspects of the isoxaben-induced CWD response. The observation that *sub-9* partially suppresses reduced root length exhibited by *prc1-1* indicates that *SUB* also mediates a CWD response that is caused by a genetic reduction in cellulose content. Thus, the collective data support the notion that the origin of the CWD relates to the reduced production of cellulose, a major carbohydrate component of the cell wall, and that *SUB* contributes to the compensatory cellular response to this type of cell-wall-related stress.

The data indicate that *SUB* already affects the early response to isoxaben-induced CWD, in particular ROS production. Previous results had revealed that the isoxaben-induced CWD response involves *THE1*-dependent ROS production [37,63]. In luminol-based extracellular ROS assays involving entire seedlings ROS production could be detected after around three to four hours following the application of isoxaben [63]. We used the intracellular ROS probe H$_2$CDFDA and a microscope-based method that enabled tissue-level resolution. H$_2$CDFDA has for example been used to assess basal intracellular ROS levels when studying *GLYCERALDEHYDE-3-PHOSPHATE DEHYDROGENASE* (*GAPDH*) genes and root hairs [55,56]. Our time-course data indicate that isoxaben induces the formation of intracellular ROS in the root meristem within 30 minutes. To our knowledge the isoxaben-dependent change in H$_2$CDFDA fluorescence signal represents the earliest available marker for the isoxaben-induced CWD response. It also indicates that this response occurs even earlier than previously appreciated [34].

The results suggest that *SUB* is required for full induction of several marker genes, such as *CCR1*, *PDF1.2*, or *RBOHD*. Moreover, the data indicate that *SUB* promotes CBI-induced accumulation of lignin and callose. The isoxaben-induced CWD response is sensitive to turgor pressure as for example induction of marker gene expression or lignin accumulation is strongly reduced upon exposing seedlings to isoxaben in combination with an osmoticum,

such as sorbitol [34,37]. It has been proposed that a mechanical stimulus initiates the CWD response to the isoxaben-induced reduction in cellulose and the associated weakening of the cellulose framework counteracting turgor pressure [34,64–67]. In this model, the stimulus could derive from a displacement or distortion of the plasma membrane relative to the cell wall. Indeed, we did not observe an obvious influence of *SUB* on the reduced lignin and callose state that results from simultaneous application of sorbitol and isoxaben indicating that *SUB* mediates a response that also depends on turgor pressure. Thus, the combined results fulfil the criteria that have been established for a CBI-induced CWD response [34,37].

Interestingly, different loss-of-function (*sub-1*, *sub-9*, *sub-21*) or gain-of-function (*pUBQ*::*SUB*:*mCherry*) mutants show reciprocal effects regarding lignin and callose accumulation, with *sub* mutants showing less and *pUBQ*::*SUB*:*mCherry* lines exhibiting higher levels of lignin or callose, respectively, upon application of isoxaben. The pUBQ::SUB:mCherry O3 and L1 lines originate from independent transformation events. They differ in their combined *SUB* and *SUB*:*mCherry* transcript levels with line O3 showing higher levels compared to line L1 (S2 Fig). Still, upon exposure to isoxaben line L1 exhibited stronger lignin and callose accumulation than line O3. This finding may be indicative of an optimal range of *SUB* activity with respect to the control of lignin and callose accumulation upon isoxaben-induced CWD. Based on this evidence, we propose the model that *SUB* represents an important genetic regulator of isoxaben-induced lignin and callose accumulation and thus cell wall composition.

Several lines of evidence indicate that *SUB* plays a biologically relevant role in CWD signaling initiated by a reduction in cellulose content. Firstly, *SUB* attenuates isoxaben-induced cell bulging in the epidermal cells of the meristem-transition zone boundary of the root. Secondly, *SUB* facilitates root growth recovery upon transient exposure of seedlings to isoxaben. Thirdly, *SUB* is involved in root growth inhibition that is a consequence of a genetic reduction of cellulose content. In particular, root length of *sub-9 prc1-1* double mutant seedlings is less diminished in comparison to the root length of *prc1-1* single mutant seedlings. The results imply that *SUB* contributes to a compensatory response that counteracts the cellular and growth defects caused by reduced cellulose synthesis and further support the notion that *SUB* plays a central role in CBI-induced CWD signaling.

How does SUB relate to other known RK genes mediating the response to CBI-induced cell wall stress, such as *THE1* and *MIK2*? *SUB*, *THE1*, and *MIK2* all promote isoxaben-induced ectopic lignin production. The three genes are also required for full isoxaben-dependent induction of certain stress marker genes [39] (Fig 2C). However, while *THE1* and *MIK2* are both required for the induction of *CYP81F2 SUB* appears to slightly attenuate induced *CYP81F2* transcript levels. *THE1* and *MIK2* are also required for *FRK1* induction while the role of *SUB* in the regulation of this gene remains to be resolved. In addition, *THE1* and *MIK2* are necessary for isoxaben-induced JA accumulation [34,39,63], a process that apparently does not require *SUB* function. We also did not observe an effect of *THE1* on root growth recovery upon transient exposure to isoxaben. In addition, we did not find an altered hypocotyl length of *sub-9 prc1-1* in comparison to *prc1-1* indicating that *SUB* does not affect hypocotyl growth inhibition in etiolated *prc1-1* seedlings, in contrast to *THE1* [38]. At the same time, our data suggest that *SUB* contributes to root growth inhibition in *prc1-1*. However, our evidence does not support a function for *THE1* in this process, as root length of *the1-1 prc1-1* double mutants did not deviate from the root length observed for *prc1-1* single mutants. This finding also implies that the lignin accumulation in the mature root parts of *prc1-1* (suppressed in *prc1-1 the1-1* double mutants) [38] does not correlate with root growth inhibition. Finally, we did not observe the left-hand root skewing in *sub* seedlings that has been described for *mik2* mutants [39], and we failed to observe floral defects in *mik2* or *the1* mutants (S3 Fig). Taken together, the data suggest that *SUB* has both overlapping and distinct

functions with *THE1* and *MIK2*. As the most parsimonious explanation of our results, we propose that *SUB* contributes to CBI-induced cell wall damage signaling independently from *THE1* and *MIK2* signaling, however the signaling pathways downstream of the different cell surface receptor kinases eventually partially converge and contribute to a subset of overlapping downstream responses.

QKY represents a central genetic component of *SUB*-mediated signal transduction during tissue morphogenesis and root hair patterning [51]. The expression patterns of *QKY* and *SUB* fully overlap [50] and present evidence supports the notion that SUB and QKY are part of a protein complex with QKY likely acting upstream to, or in parallel with, SUB [50,59,60]. However, genetic and whole-genome transcriptomic data suggested that *SUB* and *QKY* also play distinct roles during floral development [51]. The data presented in this study reveal that *SUB* and *QKY* both contribute to CBI-induced CWD signaling. Similar to *SUB QKY* is required for lignin accumulation. Moreover, *QKY* is also necessary for the prevention of cell bulging in the epidermal cells of the meristem-transition zone boundary of the root although the weaker phenotype of *qky-11* mutants indicates a lesser requirement for *QKY* in comparison to *SUB*. However, our data also indicate that *QKY* is not required for early ROS accumulation, marker gene induction, ectopic callose accumulation, and root growth recovery as we did not find these processes to be noticeably affected in *qky* mutants. Thus, these data provide genetic evidence that the functions of *SUB* and *QKY* only partially overlap and that *SUB* exerts CWD signaling functions that are independent of *QKY*. One way to rationalize these findings is to assume that SUB can also function in isolation or in protein complexes or pathways that do not involve QKY.

The diverse functions of *SUB* in development and the CWD response are likely to be achieved through participation in different signaling pathways. It is not uncommon that RKs play important roles in several biological processes. In this respect, SUB resembles for example the RK BRASSINOSTEROID INSENSITIVE 1-ASSOCIATED KINASE 1 (BAK1) / SOMA TIC EMBROYGENESIS RECEPTOR KINASE 3 (SERK3), which functions in growth, development, and plant defense [68,69]. BAK1 interacts with a range of different LRR-RKs, including FLAGELLIN SENSING 2 (FL2) and BRASSINOSTEROID INSENSITIVE 1 (BRI1), and the discrimination between the growth and immunity functions of BAK1 was recently shown to rely on phosphorylation-dependent regulation [70,71]. In light of these considerations it is reasonable to propose that SUB is a member of different receptor complexes. As kinase activity of SUB is not required for its function [44] SUB could act as a scaffold around which the components of the various complexes assemble. A scaffold role has for example been proposed for the RK AtCERK1/OsCERK1 in chitin signaling or the RK FER in immune signaling [72,73]. It will be interesting to explore this notion in future work.

Materials and methods

Plant work, plant genetics and plant transformation

Arabidopsis thaliana (L.) Heynh. var. Columbia (Col-0) and var. Landsberg (*erecta* mutant) (L*er*) were used as wild-type strains. Plants were grown as described earlier [51]. The *sub-1*, *qky-8* (all in L*er*), and the *sub-9* and *qky-11* mutants (Col) have been characterized previously [44,47,50,51]. The *prc1-1* [27], *the1-1* [38], *the1-6* [74], *mik2-1* [39], *mik2-3* [75], and *ixr2-1* [30] alleles were also described previously. The *sub-21* (Col) allele was generated using a CRISPR/Cas9 system in which the egg cell-specific promoter pEC1.2 controls Cas9 expression [76]. The single guide RNA (sgRNA) 5'-TAATAACTTGTATATCAACTT-3' binds to the region +478 to +499 of the *SUB* coding sequence. The sgRNA was designed according to the guidelines outlined in [77]. The mutant carries a frameshift mutation at position 495 relative to the *SUB* start AUG, which was verified by sequencing. The resulting predicted short SUB

protein comprises 67 amino acids. The first 39 amino acids correspond to SUB and include its predicted signal peptide of 29 residues, while amino acids 40 to 67 represent an aberrant amino acid sequence. The pUBQ::gSUB:mCherry plasmid used to generate the *SUB* overexpression lines L1 and O3 was generated previously [50]. Wild-type, and *sub* mutant plants were transformed with different constructs using Agrobacterium strain GV3101/pMP 90 [78] and the floral dip method [79]. Transgenic T1 plants were selected on Kanamycin (50 µg/ml), Hygromycin (20 µg/ml) or Glufosinate (Basta) (10 µg/ml) plates and transferred to soil for further inspection.

Cellulose quantification

Seedlings were grown on square plates with half strength MS medium and 0.3% sucrose supplemented with 0.9% agar for seven days. Cellulose content was measured following the Updegraff method essentially as described [80,81], with minor modifications as outlined here. Following the acetic nitric treatment described in [80], samples were allowed to cool at room temperature and transferred into 2 ml Eppendorf safety lock tubes. Samples were then centrifuged at 14000 rpm at 15°C for 15 min. The acetic nitric reagent was removed carefully without disturbing the pelleted material at the bottom of the tube. 1 ml of double-distilled H_2O was added, and the sample was left on the bench for 10 min at room temperature followed by centrifugation at 14000 rpm at 15°C for 15 min. After aspirating off the H_2O 1 ml acetone was added and the samples were incubated for another 15 min, followed by centrifugation at 14000 rpm at 15°C for 15 min. Afterwards acetone was removed, and samples were air-dried overnight. Then the protocol was continued as described in [80].

PCR-based gene expression analysis

For quantitative real-time PCR (qPCR) of *CesA* and stress marker genes 35 to 40 seedlings per flask were grown in liquid culture under continuous light at 18°C for seven days followed by treatment with mock or 600 nM isoxaben for eight hours or on plates (21°C, long-day conditions). With minor changes, RNA extraction and quality control were performed as described previously [82]. cDNA synthesis, qPCR, and analysis were done essentially as described [83]. Primers are listed in S1 Table.

ROS, lignin, and callose staining

Intracellular ROS accumulation in root meristems was estimated using the H_2DCFDA fluorescent stain essentially as described [56]. Seeds were grown on square plates with half strength MS medium and 1% sucrose supplemented with 0.9% agar. The seeds were stratified for two days at 4°C and incubated for seven days at 22°C under long day conditions, at a 10-degree inclined position. Seven days-old seedlings were first transferred into multi-well plates containing half strength liquid MS medium supplemented with 1% sucrose for two hours. Then medium was exchanged with liquid medium containing either DMSO (mock) or 600nM isoxaben without disturbing seedlings. 10 min prior to each time point seedlings were put in the dark and the liquid medium was supplemented with 100 µM H_2DCFDA staining solution. Images was acquired with a confocal microscope. For quantification a defined region of interest (ROI) located 500 µm above the root tip (excluding the root cap) was used in all samples. Staining for lignin (phloroglucinol) and callose (aniline blue) was performed as described in [39] and [57], respectively. ROS, phloroglucinol and aniline blue staining was quantified on micrographs using ImageJ software [84].

JA measurements

Chemicals. Jasmonic acid-d_0 and jasmonic acid-d_5 were obtained from Santa Cruz Biotechnology, Inc. (Dallas, TX, USA). Formic acid was obtained from Merck (Darmstadt, Germany), ethyl acetate and acetonitrile (LC-MS grade) were obtained from Honeywell (Seelze, Germany). Water used for chromatographic separations was purified with an AQUA-Lab—B30—Integrity system (AQUA-Lab, Ransbach-Baubach, Germany).

Sample preparation. Approximately 35 to 40 seedlings per flask were grown in liquid culture (1/2 MS, 0.3% sucrose) under continuous light and 18°C for seven days followed by treatment with mock or 600 nM isoxaben for seven hours and harvesting in liquid nitrogen. The grinded plant material (100–200 mg) was placed in a 2 mL bead beater tube (CKMix-2 mL, Bertin Technologies, Montigny-le-Bretonneux, France), filled with ceramic balls (zirconium oxide; mix beads of 1.4 mm and 2.8 mm), and an aliquot (20 μL) of a solution of acetonitrile containing the internal standard (-)*trans*-jasmonic acid-d_5 (25 μg/mL), was added. After incubation for 30 min at room temperature, the tube was filled with ice-cold ethyl acetate (1 mL). After extractive grinding (3 × 20 s with 40 s breaks; 6000 rpm) using the bead beater (Precellys Homogenizer, Bertin Technologies, Montigny-le-Bretonneux, France), the supernatant was membrane filtered (0.45 μm), evaporated to dryness (Christ RVC 2-25 CD *plus*, Martin Christ Gefriertrocknungsanlagen GmbH, Osterode am Harz, Germany), resolved in acetonitrile (70 μL) and injected into the LC–MS/MS-system (2 μL).

Liquid chromatography-triple quadrupole mass spectrometry (LC–MS/MS). Phytohormone concentrations were measured by means of UHPLC-MS/MS using a QTRAP 6500 + mass spectrometer (Sciex, Darmstadt, Germany) in the multiple reaction monitoring (MRM) mode. Positive ions were detected at an ion spray voltage at 5500 V (ESI+) and the following ion source parameters: temperature (550°C), gas 1 (55 psi), gas 2 (65 psi), curtain gas (35 psi), entrance potential (10 V) and collision activated dissociation (3 V). The temperature of the column oven was adjusted to 40°C. For plant hormone analysis, the MS/MS parameters of the compounds were tuned to achieve fragmentation of the [M+H]+ molecular ions into specific product ions: (-)trans-jasmonic acid-d_0 211→133 (quantifier) and 211→151 (qualifier), (-)trans-jasmonic acid-d_5 216→155 (quantifier) and 216→173 (qualifier). For the tuning of the mass spectrometer, solutions of the analyte and the labelled internal standard (solved in acetonitrile:water, 1:1) were introduced into the MS system by means of flow injection using a syringe pump. Separation of all samples was carried out by means of an ExionLC UHPLC (Shimadzu Europa GmbH, Duisburg, Germany), consisting of two LC pump systems (ExionLC AD), an ExionLC degasser, an ExionLC AD autosampler, an ExionLC AC column oven– 240 V and an ExionLC controller. After sample injection (2 μL), chromatography was carried out on an analytical Kinetex F5 column (100 × 2.1 mm^2, 100 Å, 1.7 μm, Phenomenex, Aschaffenburg, Germany). Chromatography was performed with a flow rate of 0.4 mL/min using 0.1% formic acid in water (v/v) as solvent A and 0.1% formic acid in acetonitrile (v/v) as solvent B, and the following gradient: 0% B held for 2 min, increased in 1 min to 30% B, in 12 min to 30% B, increased in 0.5 min to 100% B, held 2 min isocratically at 100% B, decreased in 0.5 min to 0% B, held 3 min at 0% B. Data acquisition and instrumental control was performed using Analyst 1.6.3 software (Sciex, Darmstadt, Germany).

Hypocotyl and root measurements

For measuring etiolated hypocotyl length, seedlings were grown for five days on half-strength MS agar supplemented with 0.3% sucrose. Seedlings were photographed and hypocotyl length was measured using ImageJ. For root growth assays, seedlings were grown for seven days in long-day conditions at 21°C on half-strength MS agar supplemented with 0.3% sucrose. Plates

were inclined at 10 degrees. Root length was measures using ImageJ. For root growth recovery assays seedlings were grown on half-strength MS agar supplemented with 0.3% sucrose. Seeds were stratified for two days followed by incubation at 21˚C in long day conditions for seven days. Plates were inclined at 10 degrees. Individual seedlings were transferred to plates containing either 0.01 percent DMSO (mock) or 600 nM isoxaben for 24 hours. After treatment, seedlings were transferred onto half-strength MS agar plates supplemented with 0.3% sucrose. The position of the root tip was marked under a dissection microscope. Root length was measured every 24 hours for up to three days. For root cell bulging assays seedlings were grown for seven days in long-day conditions at 21˚C on half-strength MS agar supplemented with 0.3% sucrose. Plates were inclined at 10 degrees. Individual seedlings were first transferred into liquid medium for two hours habituation followed by treatment with 600 nM isoxaben for up to seven hours. To take images, seedlings were stained with 4 µM FM4-64 for 10 minutes and imaged using confocal microscopy. Confocal micrographs were acquired at each time point. All hypocotyl length or root measurements were performed in double-blind fashion.

Statistics

Statistical analysis was performed with PRISM8 software (GraphPad Software, San Diego, USA).

Microscopy and art work

Images of seedlings exhibiting phloroglucinol staining were taken on a Leica MZ16 stereo microscope equipped with a Leica DFC320 digital camera. Images of hypocotyl and root length were taken on a Leica SAPO stereo microscope equipped with a Nikon Coolpix B500 camera. Aniline blue-stained cotyledons and root cell bulging were imaged with an Olympus FV1000 setup using an inverted IX81 stand and FluoView software (FV10-ASW version 01.04.00.09) (Olympus Europa GmbH, Hamburg, Germany) equipped with a 10x objective (NA 0.3). For assessing cell bulging a projection of a 5 µm z-stack encompassing seven individual optical sections was used. Aniline blue fluorescence was excited at 405 nm using a diode laser and detected at 425 to 525 nm. H_2DCFDA and EGFP fluorescence excitation was done at 488 nm using a multi-line argon laser and detected at 502 to 536 nm. For the direct comparisons of fluorescence intensities, laser, pinhole and gain settings of the confocal microscope were kept identical when capturing the images from the seedlings of different treatments. Scan speeds were set at 400 Hz and line averages at between 2 and 4. Measurements on digital micrographs were done using ImageJ software [84]. Images were adjusted for color and contrast using Adobe Photoshop 2020 software (Adobe, San Jose, USA).

Supporting information

S1 Fig. *SUB* **effects on isoxaben-induced marker gene expression.** Gene expression levels of several CBI marker genes by qPCR upon exposure of seven-day-old seedlings to 600 nM isoxaben for eight hours. The results from five biological replicates are shown. Marker genes and genotypes are indicated. Mean ± SD is presented. Asterisks represent adjusted P values (∗∗ $P < 0.009$, ∗∗∗ $P = 0.0002$, ∗∗∗∗ $P < 0.0001$, ns: not significant; one-way ANOVA followed by Tukey's multiple comparison tests). For all genotypes the differences between isoxaben and mock treatments were statistically significant (adjusted P value < 0.0001). Differences between mock treated wild-type and *sub-9* samples were not statistically significant. The experiment was repeated twice with similar results.
(TIF)

S2 Fig. Combined transcript levels of *SUB* and *SUB:mCherry* in two independent pUBQ:: SUB:mCherry lines. The results from three biological replicates are shown. Mean ± SD is presented.
(TIF)

S3 Fig. Comparison of floral phenotypes and root angle of Col-0, *sub*, *the1*, and *mik2*. (A) Upper panel: siliques. Bottom panel: open siliques revealing developing seeds. Genotypes are indicated. Note aberrant *sub-9* silique morphology and the reduced number of developing seeds in *sub-9*. Arrows indicate undeveloped seeds. (B) Root angle of nine-day-old seedlings grown in an upright position (10˚ angle relative to direction of gravity) on half-strength MS agar medium supplemented with 1% sucrose. Pictures were taken from the front of the plate. Genotypes are indicated. Note the slight slant to the left in *mik2-3*. (C) Quantification of results depicted in (B) and as described in Van der Does et al (2017) PLoS Genet 13: e1006832. Genotypes are indicated. Box and whisker plots are shown. Whisker ends mark the minimum and maximum of all the data. $16 \leq n \leq 22$. Asterisks represent adjusted P values (∗∗∗ P = 0.0001; one-way ANOVA followed by Tukey's multiple comparison tests). The experiment was performed twice. In the second experiment the root angle difference in *mik2-3* was not statistically significant. Scale bars: open siliques, 1 mm; closed siliques, 0.5 cm; roots, 1 cm.
(TIF)

S1 Table. Primers used in this study.
(DOCX)

Acknowledgments

Author Contributions

Conceptualization: Ajeet Chaudhary, Kay Schneitz.

Formal analysis: Ajeet Chaudhary, Xia Chen, Corinna Dawid, Kay Schneitz.

Funding acquisition: Corinna Dawid, Kay Schneitz.

Investigation: Ajeet Chaudhary, Xia Chen, Jin Gao, Barbara Leśniewska, Richard Hammerl.

Methodology: Ajeet Chaudhary.

Project administration: Kay Schneitz.

Supervision: Kay Schneitz.

Writing – original draft: Kay Schneitz.

Writing – review & editing: Corinna Dawid, Kay Schneitz.

References

1. Lampugnani ER, Khan GA, Somssich M, Persson S (2018) Building a plant cell wall at a glance. J Cell Sci 131:

2. Höfte H, Voxeur A (2017) Plant cell walls. Curr Biol 27: R865–R870. https://doi.org/10.1016/j.cub.2017.05.025 PMID: 28898654

3. Cosgrove DJ (2016) Plant cell wall extensibility: connecting plant cell growth with cell wall structure, mechanics, and the action of wall-modifying enzymes. J Exp Bot 67: 463–476. https://doi.org/10.1093/jxb/erv511 PMID: 26608646

4. Boller T, Felix G (2009) A renaissance of elicitors: perception of microbe-associated molecular patterns and danger signals by pattern-recognition receptors. Annu Rev Plant Biol 60: 379–406. https://doi.org/10.1146/annurev.arplant.57.032905.105346 PMID: 19400727

5. Franck CM, Westermann J, Boisson-Dernier A (2018) Plant malectin-like receptor kinases: from cell wall integrity to immunity and beyond. Annu Rev Plant Biol 69: 301–328. https://doi.org/10.1146/annurev-arplant-042817-040557 PMID: 29539271

6. Herger A, Dünser K, Kleine-Vehn J, Ringli C (2019) Leucine-rich repeat extensin proteins and their role in cell wall sensing. Curr Biol 29: R851–R858. https://doi.org/10.1016/j.cub.2019.07.039 PMID: 31505187

7. Vaahtera L, Schulz J, Hamann T (2019) Cell wall integrity maintenance during plant development and interaction with the environment. Nat Plants 5: 924–932. https://doi.org/10.1038/s41477-019-0502-0 PMID: 31506641

8. Wolf S (2017) Plant cell wall signalling and receptor-like kinases. Biochem J 474: 471–492. https://doi.org/10.1042/BCJ20160238 PMID: 28159895

9. Voxeur A, Höfte H (2016) Cell wall integrity signaling in plants: "To grow or not to grow that's the question". Glycobiology 26: 950–960. https://doi.org/10.1093/glycob/cww029 PMID: 26945038

10. Wolf S, van der Does D, Ladwig F, Sticht C, Kolbeck A, Schurholz AK et al. (2014) A receptor-like protein mediates the response to pectin modification by activating brassinosteroid signaling. Proc Natl Acad Sci U S A 111: 15261–15266. https://doi.org/10.1073/pnas.1322979111 PMID: 25288746

11. Wolf S, Mravec J, Greiner S, Mouille G, Höfte H (2012) Plant cell wall homeostasis is mediated by brassinosteroid feedback signaling. Curr Biol 22: 1732–1737. https://doi.org/10.1016/j.cub.2012.07.036 PMID: 22885061

12. Escobar-Restrepo JM, Huck N, Kessler S, Gagliardini V, Gheyselinck J, Yang WC et al. (2007) The FERONIA receptor-like kinase mediates male-female interactions during pollen tube reception. Science 317: 656–660. https://doi.org/10.1126/science.1143562 PMID: 17673660

13. Dünser K, Gupta S, Herger A, Feraru MI, Ringli C, Kleine-Vehn J (2019) Extracellular matrix sensing by FERONIA and Leucine-Rich Repeat Extensins controls vacuolar expansion during cellular elongation in *Arabidopsis thaliana*. EMBO J 38:

14. Feng W, Kita D, Peaucelle A, Cartwright HN, Doan V, Duan Q et al. (2018) The FERONIA receptor kinase maintains cell-wall integrity during salt stress through Ca2+ signaling. Curr Biol 28: 666–675.e5. https://doi.org/10.1016/j.cub.2018.01.023 PMID: 29456142

15. Boisson-Dernier A, Roy S, Kritas K, Grobei MA, Jaciubek M, Schroeder JI et al. (2009) Disruption of the pollen-expressed FERONIA homologs ANXUR1 and ANXUR2 triggers pollen tube discharge. Development 136: 3279–3288. https://doi.org/10.1242/dev.040071 PMID: 19736323

16. Franck C, Westermann J, Bürssner S, Lentz R, Lituiev DS, Boisson-Dernier A (2018) The protein phosphatases ATUNIS1 and ATUNIS2 regulate cell wall integrity in tip-growing cells. Plant Cell 30: 1906–1923. https://doi.org/10.1105/tpc.18.00284 PMID: 29991535

17. Mecchia MA, Santos-Fernandez G, Duss NN, Somoza SC, Boisson-Dernier A, Gagliardini V et al. (2017) RALF4/19 peptides interact with LRX proteins to control pollen tube growth in Arabidopsis. Science 358: 1600–1603. https://doi.org/10.1126/science.aao5467 PMID: 29242232

18. Miyazaki S, Murata T, Sakurai-Ozato N, Kubo M, Demura T, Fukuda H et al. (2009) ANXUR1 and 2, sister genes to FERONIA/SIRENE, are male factors for coordinated fertilization. Curr Biol 19: 1327–1331. https://doi.org/10.1016/j.cub.2009.06.064 PMID: 19646876

19. Bai L, Ma X, Zhang G, Song S, Zhou Y, Gao L et al. (2014) A receptor-like kinase mediates ammonium homeostasis and is important for the polar growth of root hairs in *Arabidopsis*. Plant Cell 26: 1497–1511. https://doi.org/10.1105/tpc.114.124586 PMID: 24769480

20. Haruta M, Sabat G, Stecker K, Minkoff BB, Sussman MR (2014) A peptide hormone and its receptor protein kinase regulate plant cell expansion. Science 343: 408–411. https://doi.org/10.1126/science.1244454 PMID: 24458638

21. Schoenaers S, Balcerowicz D, Breen G, Hill K, Zdanio M, Mouille G et al. (2018) The auxin-regulated CrRLK1L kinase ERULUS controls cell wall composition during root hair tip growth. Curr Biol 28: 722–732.e6. https://doi.org/10.1016/j.cub.2018.01.050 PMID: 29478854

22. Somerville C, Bauer S, Brininstool G, Facette M, Hamann T, Milne J et al. (2004) Toward a systems approach to understanding plant cell walls. Science 306: 2206–2211. https://doi.org/10.1126/science.1102765 PMID: 15618507

23. Caño-Delgado A, Penfield S, Smith C, Catley M, Bevan M (2003) Reduced cellulose synthesis invokes lignification and defense responses in *Arabidopsis thaliana*. Plant J 34: 351–362. https://doi.org/10.1046/j.1365-313x.2003.01729.x PMID: 12713541

24. Cano-Delgado AI, Metzlaff K, Bevan MW (2000) The *eli1* mutation reveals a link between cell expansion and secondary cell wall formation in *Arabidopsis thaliana*. Development 127: 3395–3405. PMID: 10887094

25. Ellis C, Karafyllidis I, Wasternack C, Turner JG (2002) The Arabidopsis mutant cev1 links cell wall signaling to jasmonate and ethylene responses. Plant Cell 14: 1557–1566. https://doi.org/10.1105/tpc.002022 PMID: 12119374

26. Ellis C, Turner JG (2001) The Arabidopsis mutant *cev1* has constitutively active jasmonate and ethylene signal pathways and enhanced resistance to pathogens. Plant Cell 13: 1025–1033. https://doi.org/10.1105/tpc.13.5.1025 PMID: 11340179

27. Fagard M, Desnos T, Desprez T, Goubet F, Refregier G, Mouille G et al. (2000) *PROCUSTE1* encodes a cellulose synthase required for normal cell elongation specifically in roots and dark-grown hypocotyls of Arabidopsis. Plant Cell 12: 2409–2424. https://doi.org/10.1105/tpc.12.12.2409 PMID: 11148287

28. Heim DR, Skomp JR, Tschabold EE, Larrinua IM (1990) Isoxaben inhibits the synthesis of acid insoluble cell wall materials in *Arabidopsis thaliana*. Plant Physiol 93: 695–700. https://doi.org/10.1104/pp.93.2.695 PMID: 16667525

29. Lefebvre A, Maizonnier D, Gaudry JC, Clair D, Scalla R (1987) Some effects of the herbicide EL-107 on cellular growth and metabolism. Weed Research 27: 125–134.

30. Desprez T, Vernhettes S, Fagard M, Refrégier G, Desnos T, Aletti E et al. (2002) Resistance against herbicide isoxaben and cellulose deficiency caused by distinct mutations in same cellulose synthase isoform CESA6. Plant Physiol 128: 482–490. https://doi.org/10.1104/pp.010822 PMID: 11842152

31. Scheible WR, Eshed R, Richmond T, Delmer D, Somerville C (2001) Modifications of cellulose synthase confer resistance to isoxaben and thiazolidinone herbicides in *Arabidopsis lxr1* mutants. Proc Natl Acad Sci U S A 98: 10079–10084. https://doi.org/10.1073/pnas.191361598 PMID: 11517344

32. Paredez AR, Somerville CR, Ehrhardt DW (2006) Visualization of cellulose synthase demonstrates functional association with microtubules. Science 312: 1491–1495. https://doi.org/10.1126/science.1126551 PMID: 16627697

33. Heim DR, Skomp JR, Waldron C, Larrinua IM (1991) Differential response to isoxaben of cellulose biosynthesis by wild-type and resistant strains of Arabidopsis thaliana. Pestic Biochem Physiol 39: 93–99.

34. Engelsdorf T, Gigli-Bisceglia N, Veerabagu M, McKenna JF, Vaahtera L, Augstein F et al. (2018) The plant cell wall integrity maintenance and immune signaling systems cooperate to control stress responses in *Arabidopsis thaliana*. Sci Signal 11: eaao3070. https://doi.org/10.1126/scisignal.aao3070 PMID: 29945884

35. Hamann T (2015) The plant cell wall integrity maintenance mechanism—a case study of a cell wall plasma membrane signaling network. Phytochemistry 112: 100–109. https://doi.org/10.1016/j.phytochem.2014.09.019 PMID: 25446233

36. Wormit A, Butt SM, Chairam I, McKenna JF, Nunes-Nesi A, Kjaer L et al. (2012) Osmosensitive changes of carbohydrate metabolism in response to cellulose biosynthesis inhibition. Plant Physiol 159: 105–117. https://doi.org/10.1104/pp.112.195198 PMID: 22422940

37. Hamann T, Bennett M, Mansfield J, Somerville C (2009) Identification of cell-wall stress as a hexose-dependent and osmosensitive regulator of plant responses. Plant J 57: 1015–1026. https://doi.org/10.1111/j.1365-313X.2008.03744.x PMID: 19036034

38. Hématy K, Sado PE, Van Tuinen A, Rochange S, Desnos T, Balzergue S et al. (2007) A receptor-like kinase mediates the response of *Arabidopsis* cells to the inhibition of cellulose synthesis. Curr Biol 17: 922–931. https://doi.org/10.1016/j.cub.2007.05.018 PMID: 17540573

39. Van der Does D, Boutrot F, Engelsdorf T, Rhodes J, McKenna JF, Vernhettes S et al. (2017) The Arabidopsis leucine-rich repeat receptor kinase MIK2/LRR-KISS connects cell wall integrity sensing, root growth and response to abiotic and biotic stresses. PLoS Genet 13: e1006832. https://doi.org/10.1371/journal.pgen.1006832 PMID: 28604776

40. Julkowska M, Koevoets IT, Mol S, Hoefsloot HC, Feron R, Tester M et al. (2017) Genetic components of root architecture remodeling in response to salt stress. Plant Cell 29: 3198–3213. https://doi.org/10.1105/tpc.16.00680 PMID: 29114015

41. Wang T, Liang L, Xue Y, Jia PF, Chen W, Zhang MX et al. (2016) A receptor heteromer mediates the male perception of female attractants in plants. Nature 531: 241–244. https://doi.org/10.1038/nature16975 PMID: 26863186

42. Xu SL, Rahman A, Baskin TI, Kieber JJ (2008) Two leucine-rich repeat receptor kinases mediate signaling, linking cell wall biosynthesis and ACC synthase in *Arabidopsis*. Plant Cell 20: 3065–3079. https://doi.org/10.1105/tpc.108.063354 PMID: 19017745

43. Gonneau M, Desprez T, Martin M, Doblas VG, Bacete L, Miart F et al. (2018) Receptor kinase THESEUS1 is a Rapid Alkalinization Factor 34 receptor in *Arabidopsis*. Curr Biol 28: 2452–2458.e4. https://doi.org/10.1016/j.cub.2018.05.075 PMID: 30057301

44. Chevalier D, Batoux M, Fulton L, Pfister K, Yadav RK, Schellenberg M et al. (2005) STRUBBELIG defines a receptor kinase-mediated signaling pathway regulating organ development in *Arabidopsis*. Proc Natl Acad Sci U S A 102: 9074–9079. https://doi.org/10.1073/pnas.0503526102 PMID: 15951420

45. Kwak SH, Shen R, Schiefelbein J (2005) Positional signaling mediated by a receptor-like kinase in Arabidopsis. Science 307: 1111–1113. https://doi.org/10.1126/science.1105373 PMID: 15618487

46. Lin L, Zhong SH, Cui XF, Li J, He ZH (2012) Characterization of temperature-sensitive mutants reveals a role for receptor-like kinase SCRAMBLED/STRUBBELIG in coordinating cell proliferation and differentiation during Arabidopsis leaf development. Plant J 72: 707–720. https://doi.org/10.1111/j.1365-313X.2012.05109.x PMID: 22805005

47. Vaddepalli P, Fulton L, Batoux M, Yadav RK, Schneitz K (2011) Structure-function analysis of STRUBBELIG, an Arabidopsis atypical receptor-like kinase involved in tissue morphogenesis. PLoS One 6: e19730. https://doi.org/10.1371/journal.pone.0019730 PMID: 21603601

48. Sager RE, Lee JY (2018) Plasmodesmata at a glance. J Cell Sci 131: jcs209346. https://doi.org/10.1242/jcs.209346 PMID: 29880547

49. Otero S, Helariutta Y, Benitez-Alfonso Y (2016) Symplastic communication in organ formation and tissue patterning. Curr Opin Plant Biol 29: 21–28. https://doi.org/10.1016/j.pbi.2015.10.007 PMID: 26658335

50. Vaddepalli P, Herrmann A, Fulton L, Oelschner M, Hillmer S, Stratil TF et al. (2014) The C2-domain protein QUIRKY and the receptor-like kinase STRUBBELIG localize to plasmodesmata and mediate tissue morphogenesis in *Arabidopsis thaliana*. Development 141: 4139–4148. https://doi.org/10.1242/dev.113878 PMID: 25256344

51. Fulton L, Batoux M, Vaddepalli P, Yadav RK, Busch W, Andersen SU et al. (2009) *DETORQUEO*, *QUIRKY*, and *ZERZAUST* represent novel components involved in organ development mediated by the receptor-like kinase STRUBBELIG in *Arabidopsis thaliana*. PLoS Genet 5: e1000355. https://doi.org/10.1371/journal.pgen.1000355 PMID: 19180193

52. Vaddepalli P, Fulton L, Wieland J, Wassmer K, Schaeffer M, Ranf S et al. (2017) The cell wall-localized atypical β-1,3 glucanase ZERZAUST controls tissue morphogenesis in *Arabidopsis thaliana*. Development 144: 2259–2269. https://doi.org/10.1242/dev.152231 PMID: 28507000

53. Desprez T, Juraniec M, Crowell EF, Jouy H, Pochylova Z, Parcy F et al. (2007) Organization of cellulose synthase complexes involved in primary cell wall synthesis in *Arabidopsis thaliana*. Proc Natl Acad Sci U S A 104: 15572–15577. https://doi.org/10.1073/pnas.0706569104 PMID: 17878303

54. Persson S, Paredez A, Carroll A, Palsdottir H, Doblin M, Poindexter P et al. (2007) Genetic evidence for three unique components in primary cell-wall cellulose synthase complexes in *Arabidopsis*. Proc Natl Acad Sci U S A 104: 15566–15571. https://doi.org/10.1073/pnas.0706592104 PMID: 17878302

55. Henry E, Fung N, Liu J, Drakakaki G, Coaker G (2015) Beyond glycolysis: GAPDHs are multi-functional enzymes involved in regulation of ros, autophagy, and plant immune responses. PLoS Genet 11: e1005199. https://doi.org/10.1371/journal.pgen.1005199 PMID: 25918875

56. Juárez SP, Mangano S, Estevez JM (2015) Improved ROS measurement in root hair cells. Methods Mol Biol 1242: 67–71. https://doi.org/10.1007/978-1-4939-1902-4_6 PMID: 25408444

57. Schenk ST, Schikora A (2015) Staining of callose depositions in root and leaf tissues. Bio-protocol 5: e1429.

58. Heim DR, Roberts JL, Pike PD, Larrinua IM (1990) A second locus, *Ixr*B1 in *Arabidopsis thaliana*, that confers resistance to the herbicide isoxaben. Plant Physiol 92: 858–861. https://doi.org/10.1104/pp.92.3.858 PMID: 16667361

59. Trehin C, Schrempp S, Chauvet A, Berne-Dedieu A, Thierry AM, Faure JE et al. (2013) QUIRKY interacts with STRUBBELIG and PAL OF QUIRKY to regulate cell growth anisotropy during Arabidopsis gynoecium development. Development 140: 4807–4817. https://doi.org/10.1242/dev.091868 PMID: 24173806

60. Song JH, Kwak SH, Nam KH, Schiefelbein J, Lee MM (2019) QUIRKY regulates root epidermal cell patterning through stabilizing SCRAMBLED to control CAPRICE movement in *Arabidopsis*. Nat Commun 10: 1744. https://doi.org/10.1038/s41467-019-09715-8 PMID: 30988311

61. Sampathkumar A, Yan A, Krupinski P, Meyerowitz EM (2014) Physical forces regulate plant development and morphogenesis. Curr Biol 24: R475–83. https://doi.org/10.1016/j.cub.2014.03.014 PMID: 24845680

62. Kwak SH, Woo S, Lee MM, Schiefelbein J (2014) Distinct signaling mechanisms in multiple developmental pathways by the SCRAMBLED receptor of Arabidopsis. Plant Physiol 166: 976–987. https://doi.org/10.1104/pp.114.247288 PMID: 25136062

63. Denness L, McKenna JF, Segonzac C, Wormit A, Madhou P, Bennett M et al. (2011) Cell wall damage-induced lignin biosynthesis is regulated by a reactive oxygen species- and jasmonic acid-dependent process in Arabidopsis. Plant Physiol 156: 1364–1374. https://doi.org/10.1104/pp.111.175737 PMID: 21546454

64. Kohorn BD, Kobayashi M, Johansen S, Riese J, Huang LF, Koch K et al. (2006) An Arabidopsis cell wall-associated kinase required for invertase activity and cell growth. Plant J 46: 307–316. https://doi.org/10.1111/j.1365-313X.2006.02695.x PMID: 16623892

65. Engelsdorf T, Hamann T (2014) An update on receptor-like kinase involvement in the maintenance of plant cell wall integrity. Ann Bot 114: 1339–1347. https://doi.org/10.1093/aob/mcu043 PMID: 24723447

66. Haswell ES, Verslues PE (2015) The ongoing search for the molecular basis of plant osmosensing. J Gen Physiol 145: 389–394. https://doi.org/10.1085/jgp.201411295 PMID: 25870206

67. Nissen KS, Willats WGT, Malinovsky FG (2016) Understanding CrRLK1L function: cell walls and growth control. Trends Plant Sci 21: 516–527. https://doi.org/10.1016/j.tplants.2015.12.004 PMID: 26778775

68. He Y, Zhou J, Shan L, Meng X (2018) Plant cell surface receptor-mediated signaling—a common theme amid diversity. J Cell Sci 131: 1–11.

69. Ma X, Xu G, He P, Shan L (2016) SERKing coreceptors for receptors. Trends Plant Sci 21: 1017–1033. https://doi.org/10.1016/j.tplants.2016.08.014 PMID: 27660030

70. Schwessinger B, Roux M, Kadota Y, Ntoukakis V, Sklenar J, Jones A et al. (2011) Phosphorylation-dependent differential regulation of plant growth, cell death, and innate immunity by the regulatory receptor-like kinase BAK1. PLoS Genet 7: e1002046. https://doi.org/10.1371/journal.pgen.1002046 PMID: 21593986

71. Perraki A, DeFalco TA, Derbyshire P, Avila J, Séré D, Sklenar J et al. (2018) Phosphocode-dependent functional dichotomy of a common co-receptor in plant signalling. Nature 561: 248–252. https://doi.org/10.1038/s41586-018-0471-x PMID: 30177827

72. Cao Y, Liang Y, Tanaka K, Nguyen CT, Jedrzejczak RP, Joachimiak A et al. (2014) The kinase LYK5 is a major chitin receptor in Arabidopsis and forms a chitin-induced complex with related kinase CERK1. Elife 3: e03766.

73. Stegmann M, Monaghan J, Smakowska-Luzan E, Rovenich H, Lehner A, Holton N et al. (2017) The receptor kinase FER is a RALF-regulated scaffold controlling plant immune signaling. Science 355: 287–289. https://doi.org/10.1126/science.aal2541 PMID: 28104890

74. Merz D, Richter J, Gonneau M, Sanchez-Rodriguez C, Eder T, Sormani R et al. (2017) T-DNA alleles of the receptor kinase THESEUS1 with opposing effects on cell wall integrity signaling. J Exp Bot 68: 4583–4593. https://doi.org/10.1093/jxb/erx263 PMID: 28981771

75. Coleman AD, Raasch L, Maroschek J, Ranf S, Hückelhoven R (2019) The Arabidopsis leucine-rich repeat receptor kinase MIK2 is a crucial component of pattern-triggered immunity responses to *Fusarium* fungi. bioRxiv 720037.

76. Wang ZP, Xing HL, Dong L, Zhang HY, Han CY, Wang XC et al. (2015) Egg cell-specific promoter-controlled CRISPR/Cas9 efficiently generates homozygous mutants for multiple target genes in Arabidopsis in a single generation. Genome Biol 16: 144. https://doi.org/10.1186/s13059-015-0715-0 PMID: 26193878

77. Xie K, Zhang J, Yang Y (2014) Genome-wide prediction of highly specific guide RNA spacers for CRISPR-Cas9-mediated genome editing in model plants and major crops. Mol Plant 7: 923–926. https://doi.org/10.1093/mp/ssu009 PMID: 24482433

78. Koncz C, Schell J (1986) The promoter of TL-DNA gene 5 controls the tissue-specific expression of chimaeric genes carried by a novel type of Agrobacterium binary vector. Mol Gen Genet 204: 383–396.

79. Clough SJ, Bent AF (1998) Floral dip: a simplified method for *Agrobacterium*-mediated transformation of *Arabidopsis thaliana*. Plant J 16: 735–743. https://doi.org/10.1046/j.1365-313x.1998.00343.x PMID: 10069079

80. Kumar M, Turner S (2015) Protocol: a medium-throughput method for determination of cellulose content from single stem pieces of *Arabidopsis thaliana*. Plant Methods 11: 46. https://doi.org/10.1186/s13007-015-0090-6 PMID: 26464578

81. Updegraff DM (1969) Semimicro determination of cellulose in biological materials. Anal Biochem 32: 420–424. https://doi.org/10.1016/s0003-2697(69)80009-6 PMID: 5361396

82. Box MS, Coustham V, Dean C, Mylne JS (2011) Protocol: A simple phenol-based method for 96-well extraction of high quality RNA from Arabidopsis. Plant Methods 7: 7. https://doi.org/10.1186/1746-4811-7-7 PMID: 21396125

83. Enugutti B, Kirchhelle C, Oelschner M, Torres Ruiz RA, Schliebner I, Leister D et al. (2012) Regulation of planar growth by the Arabidopsis AGC protein kinase UNICORN. Proc Natl Acad Sci U S A 109: 15060–15065. https://doi.org/10.1073/pnas.1205089109 PMID: 22927420

84. Rueden CT, Schindelin J, Hiner MC, DeZonia BE, Walter AE, Arena ET et al. (2017) ImageJ2: ImageJ for the next generation of scientific image data. BMC Bioinformatics 18: 529. https://doi.org/10.1186/s12859-017-1934-z PMID: 29187165